AD-A121 190 EXCITED STATE CHEMISTRY OF HALOGEN AZIDES(U) ROCKWELL 1/1
INTERNATIONAL THOUSAND OAKS CA SCIENCE CENTER
A T PRITT AUG 82 SC5218.4FR AFOSR-TR-82-0916
UNCLASSIFIED F49620-79-C-0053 F/G 7/4 NL

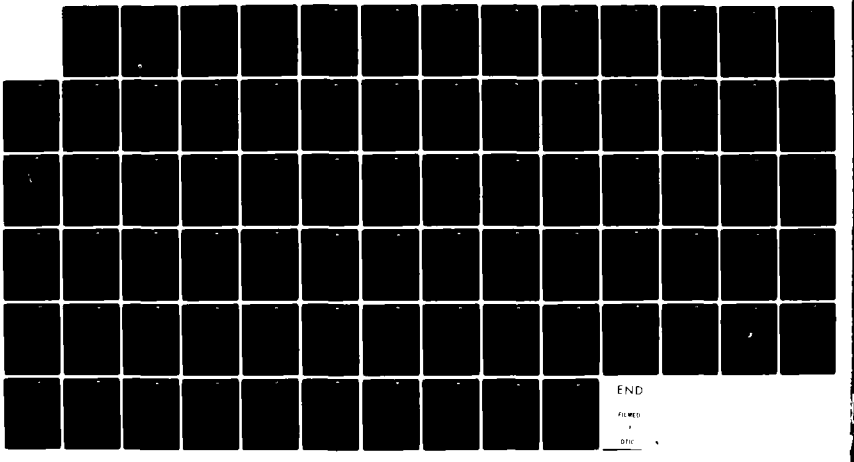

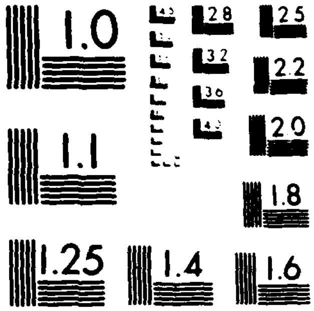

MICROCOPY RESOLUTION TEST CHART
NATIONAL BUREAU OF STANDARDS-1963-A

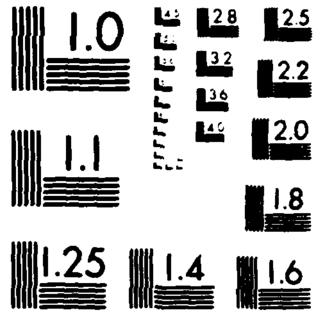

MICROCOPY RESOLUTION TEST CHART
NATIONAL BUREAU OF STANDARDS-1963-A

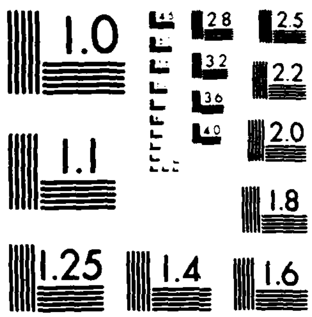

MICROCOPY RESOLUTION TEST CHART
NATIONAL BUREAU OF STANDARDS-1963-A

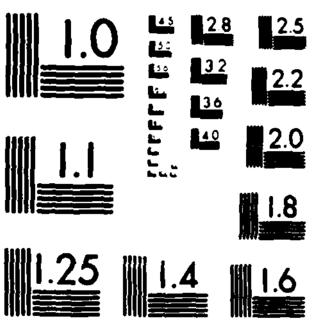

MICROCOPY RESOLUTION TEST CHART
NATIONAL BUREAU OF STANDARDS-1963-A

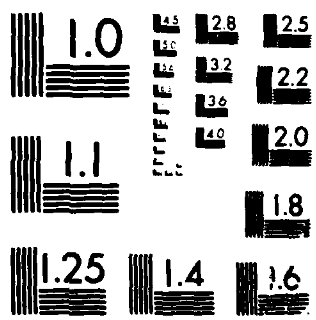

MICROCOPY RESOLUTION TEST CHART
NATIONAL BUREAU OF STANDARDS-1963-A

AFOSR-TR- 82-0916

(12)

SC5218.4FR

AD A121190

SC5218.4FR

Copy No. 7

EXCITED STATE CHEMISTRY OF HALOGEN AZIDES

FINAL REPORT FOR THE PERIOD
June 1, 1979 through May 31, 1982

CONTRACT NO. F49620-79-C-0053

Prepared for

Director of Chemical & Atmospheric Sciences
Building 410
Bolling AFB, DC 20332

A.T. Pritt, Jr.
Principal Investigator

AUGUST 1982

DTIC
ELECTE
NOV 0 8 1982
S D
E

Approved for public release; distribution unlimited

Rockwell International
Science Center

82 11 08 024

UNCLASSIFIED

SECURITY CLASSIFICATION OF THIS PAGE (When Data Entered)

REPORT DOCUMENTATION PAGE	READ INSTRUCTIONS BEFORE COMPLETING FORM
1. REPORT NUMBER: AFOSR-TR- 82-0916	2. GOVT ACCESSION NO.: AD-A121 190
3. RECIPIENT'S CATALOG NUMBER	
4. TITLE (and Subtitle): EXCITED STATE CHEMISTRY OF HALOGEN AZIDES	5. TYPE OF REPORT & PERIOD COVERED: Final Report
	6. PERFORMING ORG. REPORT NUMBER
7. AUTHOR(s): A.T. Pritt, Jr.	8. CONTRACT OR GRANT NUMBER(s): F49620-79-C-0053
9. PERFORMING ORGANIZATION NAME AND ADDRESS: Rockwell International Science Center, 1049 Camino Dos Rios, Thousand Oaks, California 91360	10. PROGRAM ELEMENT, PROJECT, TASK AREA & WORK UNIT NUMBERS: 61102F, 2303/B1
11. CONTROLLING OFFICE NAME AND ADDRESS: AFOSR, Director of Chemical & Atmospheric Sciences/NC, Building 410, Bolling AFB, DC 20332	12. REPORT DATE: August 1982
	13. NUMBER OF PAGES: 71
14. MONITORING AGENCY NAME & ADDRESS (if different from Controlling Office)	15. SECURITY CLASS. (of this report): Unclassified
	15a. DECLASSIFICATION/DOWNGRADING SCHEDULE

16. DISTRIBUTION STATEMENT (of this Report)

Approved for public release; distribution unlimited.

17. DISTRIBUTION STATEMENT (of the abstract entered in Block 20, if different from Report)

18. SUPPLEMENTARY NOTES

19. KEY WORDS (Continue on reverse side if necessary and identify by block number)

halogen azides, NF, NCl, NBr, spectroscopy, chemiluminescence, photodissociation, lasers, matrix isolation, halogen atom reactions, reaction rates, quenching rates, excited states, molecular constants.

20. ABSTRACT (Continue on reverse side if necessary and identify by block number)

A three year program directed towards understanding the behavior of excited halogen azides in photochemical system and the role of azide intermediates in elementary chemical reaction has been completed. Experiments performed are divided into four tasks as follows: (1) Chemiluminescence flow tube studies and halogen atom-azide molecule reactions, (2) UV and vacuum UV absorption spectroscopy of the ClN_3, (3) real-time, laser-initiated studies, and (4) matrix isolation studies of the F + HN_3

DD FORM 1 JAN 73 1473 EDITION OF 1 NOV 65 IS OBSOLETE

UNCLASSIFIED

SECURITY CLASSIFICATION OF THIS PAGE (When Data Entered)

reaction. The data obtained included rates of halogen atom-azide molecule reactions, mechanisms for the formation of nitrenes in the singlet states including the nature of intermediates operative in these flames, absorption spectra of ClN_3, and molecular constants for the singlet states ($b^1\Sigma^+$ and $a^1\Delta$) of NCl and NBr.

a prime delta

b prime sigma

ABSTRACT

A three year program directed towards understanding the behavior of excited halogen azides in photochemical system and the role of azide intermediates in elementary chemical reaction has been completed. Experiments performed are divided into four tasks as follows: 1) Chemilumenescence flow tube studies and halogen atom-azide molecule reactions, 2) UV and vacuum UV absorption spectroscopy of the ClN_3, 3) real-time, laser-initiated studies, and 4) matrix isolation studies of the F + HN_3 reaction. The data obtained included rates of halogen atom-azide molecule reactions, mechanisms for the formation of nitrenes in the singlet states including the nature of intermediates operative in these flames, absorption spectra of ClN_3, and molecular constants for the singlet states ($b^1\Sigma^+$ and $a^1\Delta$) of NCl and NBr.

DTIC COPY INSPECTED

Accession For
NTIS GRA&I [X]
DTIC TAB [ ]
Unannounced [ ]
Justification
By
Distribution/
Availability Codes
Dist | Avail and/or Special
A

AIR FORCE OFFICE OF SCIENTIFIC RESEARCH (AFSC)
NOTICE OF TRANSMITTAL TO DTIC
This technical report has been reviewed and is approved for public release IAW AFR 190-12.
Distribution is unlimited.
MATTHEW J. KERPER
Chief, Technical Information Division

TABLE OF CONTENTS

LIST OF FIGURES

LIST OF TABLES

INTRODUCTION

This report describes the results obtained in the program "Excited State Chemistry of the Halogen Azides" from June 1979 through May 1982 under AFOSR Contract F49620-79-C-0053. A total of six publications, of which two are in manuscript form, and six oral presentations resulted from this work.

The photochemistry of azide molecules (RN_3) has been shown to be dominated by singlet-singlet transitions leading to singlet fragments.[1-3] For the simplest member of the family, HN_3, photolysis at several wavelengths in the lower energy region of its absorption spectrum has been shown to produce electronically excited singlet NH in high yield.[3-5] This behavior can be understood in terms of conservation of electron spin, a constraint which may be quite strong for species comprised of such light atoms.

The analogous halogen azides FN_3, ClN_3, and BrN_3 are highly energetic molecules which should be similarly capable of forming electronically excited singlet NX products upon decomposition. Although the excited state chemistry of these species has been studied only to a very limited extent, there is some evidence for formation of electronically excited NX molecules from reactions in which XN_3 species may participate as intermediates. Several years ago, Clark and Clyne observed NCl* and NBr* in their excited $b^1\Sigma^+$ states from the reactions of Cl or Br atoms with ClN_3.[6] Furthermore, these authors[7] identified the presence of the azide radical, N_3, in these reaction systems and, consequently, concluded that the production of the $b^1\Sigma^+$ state occurred via the reaction,

$$X + N_3 \rightarrow NX\ (b^1\Sigma^+) + N_2 \quad . \qquad (1)$$

In the analogous $F + HN_3$ reaction, we observed production of both the $a^1\Delta$ and $b^1\Sigma^+$ states of NF; however, only the $a^1\Delta$ state scaled linearly with the limiting reagent (in this case, HN_3), whereas the majority of the NF ($b^1\Sigma^+$) was produced via second order processes.[8] In both systems, the formation of

electronically excited products can be understood in terms of excited XN_3 intermediates, which may be constrained by spin conservation to produce singlet fragments.

A schematic of the energy profile along a reacting path for reaction (1) is presented in Fig. 1. The ^2P halogen atom and $^2\Pi$ azide radical can proceed along either a singlet or triplet potential surface associated with a halogen azide intermediate. As long as the triplet potential is energetically unaccessible to the reactants, a curve crossing in the exit channel must be encountered in order to produce the $^3\Sigma^-$ state of NX. The branching ratio in forming singlet vs triplet products depends strongly on the strength and dynamics associated with this crossing zone. If the spin coupling in the crossing zone is sufficiently weak, reaction (1) can result in the preferred production of either $b^1\Sigma$ or $a^1\Delta$ state of NX. In fact, photon yield experiments on the F + HN_3 reaction indicates that the F + N_3 reaction produces NF ($a^1\Delta$) with near unit efficiency.[9] Clearly, these reactions are extremely important to current Air Force interests in developing a chemically pumped laser operating in the visible and near-infrared region of the spectrum.

The halogen azides are known to produce NX diatomics upon photolysis.[10] Apart from this basic result, little else is known about the photochemistry of these species. Although ultraviolet spectra have been recorded for ClN_3[7] and FN_3[11,12] detailed information concerning the nature of the states of the parents or photofragments has not been reported.

The goal of this program was directed towards a basic understanding of the chemistry of the halogen azides and the electronically excited NX molecules which may be formed by photolysis or chemical reaction. The program therefore centered on three aspects: 1) photochemistry of the halogen azides, 2) kinetics and mechanisms of X + HN_3 and X + N_3 reactions, and 3) excited state chemistry of the NX* products. The techniques used during the course of the program consisted of conventional steady state flow tube chemiluminesence, UV-vacuum and UV spectroscopy, time-resolve, laser-initiated fluorescence, and matrix isolation IR spectroscopy. The following section (Section III)

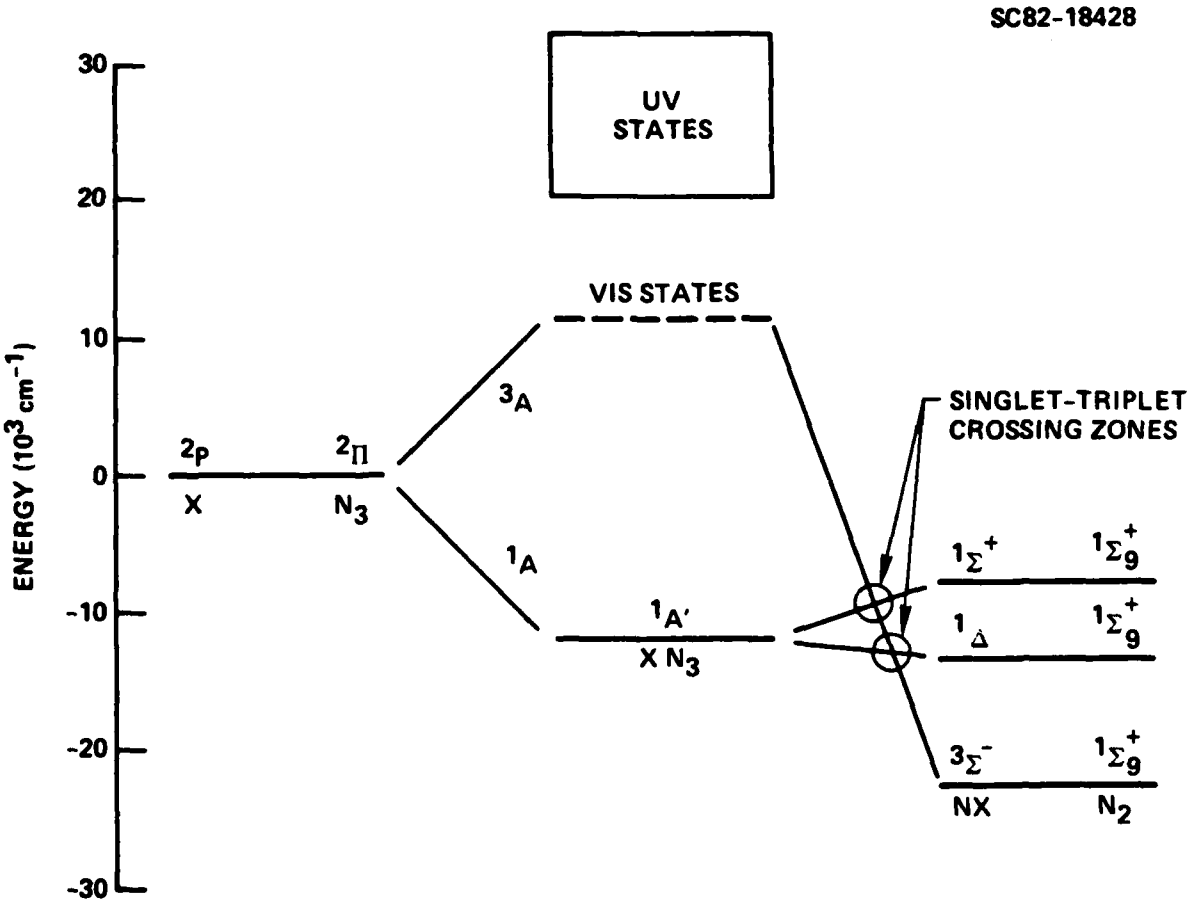

Fig. 1 Energy vs reaction path for X + N_3.

presents a description of the experiments and a brief review of the results and conclusions of these experiments.

This report reviews the work performed during the contract period. Much of this work is published or is in manuscript form given in this report as Appendix A and B. Hence, the published results and conclusions are only summarized. Sections 1.1, 1.2, 1.6, 2.1, 2.2, 3.1, 3.2, 3.3 and 3.4 have been published in the open literature, and their references are clearly stated. However, other sections contain work which has not been published due to the preliminary nature of the investigation. These nonpublished results include chemiluminescence flow tube studies of the F/Br + HN_3, F + ClN_3, and F + HNCO flames. In addition, some preliminary investigation of the nature of the intermediate using the technique of matrix isolation ir spectroscopy is reported in Section 4.

RESULTS

1. Chemiluminescence Flow Tube Studies

Much can be learned from survey style chemiluminescence experiments performed in a flow tube reaction apparatus. The primary information that can be gathered in such a flowing apparatus is the spectroscopy associated with the chemiluminescence, the mechanism by monitoring the emission intensity of selected spectral components while carefully varying material flow of reagents, the rates of the formation and decay of selected emitters from the flame time profile, and in some cases, the photon yield of the emitters with respect to the limiting reagent in the flow.

1.1 Triply Concentric Flow Tube Apparatus

The chemiluminescence flow tube was constructed from a 75 cm length of Teflon tubing 6 cm in diameter, having an inside diameter of 3.2 cm. Along the axis of this Teflon tube was a moveable double concentric tube assembly, consisting of two stainless steel tubes. The outer tube was 1.2 cm diameter and the inner, 0.6 cm diameter. The inner stainless steel tubing extended beyond the outer Teflon coated tubing by 10 cm, and this exposed portion of the smaller tube was coated with halocarbon wax. The end of the smaller tube was capped and small holes were drilled in the sides. The effect of these small holes was to spray reagents laterally to the flow of the other reactive species. A schematic of this triply concentric tube arrangement is shown in Fig. 2.

Fluorine atoms were generated by passage of F_2 or CF_4 diluted in argon through a microwave discharge (Raytheon 2450 MHz, 100 watts). Partial pressure of fluorine atoms were 50-100 mtorr with F_2 as the source, and 2-5 mtorr with CF_4 as the source. The fluorine atoms traversed the outer annulus of the flow tube assembly. In this region, all walls were Teflon. To generate other halogen atoms,the halogen containing source, which in this study was HCl, Cl_2, and Br_2, was introduced to the F-atom flow through the

RESULTS

1. Chemiluminescence Flow Tube Studies

Much can be learned from survey style chemiluminescence experiments performed in a flow tube reaction apparatus. The primary information that can be gathered in such a flowing apparatus is the spectroscopy associated with the chemiluminescence, the mechanism by monitoring the emission intensity of selected spectral components while carefully varying material flow of reagents, the rates of the formation and decay of selected emitters from the flame time profile, and in some cases, the photon yield of the emitters with respect to the limiting reagent in the flow.

1.1 Triply Concentric Flow Tube Apparatus

The chemiluminescence flow tube was constructed from a 75 cm length of Teflon tubing 6 cm in diameter, having an inside diameter of 3.2 cm. Along the axis of this Teflon tube was a moveable double concentric tube assembly, consisting of two stainless steel tubes. The outer tube was 1.2 cm diameter and the inner, 0.6 cm diameter. The inner stainless steel tubing extended beyond the outer Teflon coated tubing by 10 cm, and this exposed portion of the smaller tube was coated with halocarbon wax. The end of the smaller tube was capped and small holes were drilled in the sides. The effect of these small holes was to spray reagents laterally to the flow of the other reactive species. A schematic of this triply concentric tube arrangement is shown in Fig. 2.

Fluorine atoms were generated by passage of F_2 or CF_4 diluted in argon through a microwave discharge (Raytheon 2450 MHz, 100 watts). Partial pressure of fluorine atoms were 50-100 mtorr with F_2 as the source, and 2-5 mtorr with CF_4 as the source. The fluorine atoms traversed the outer annulus of the flow tube assembly. In this region, all walls were Teflon. To generate other halogen atoms,the halogen containing source, which in this study was HCl, Cl_2, and Br_2, was introduced to the F-atom flow through the

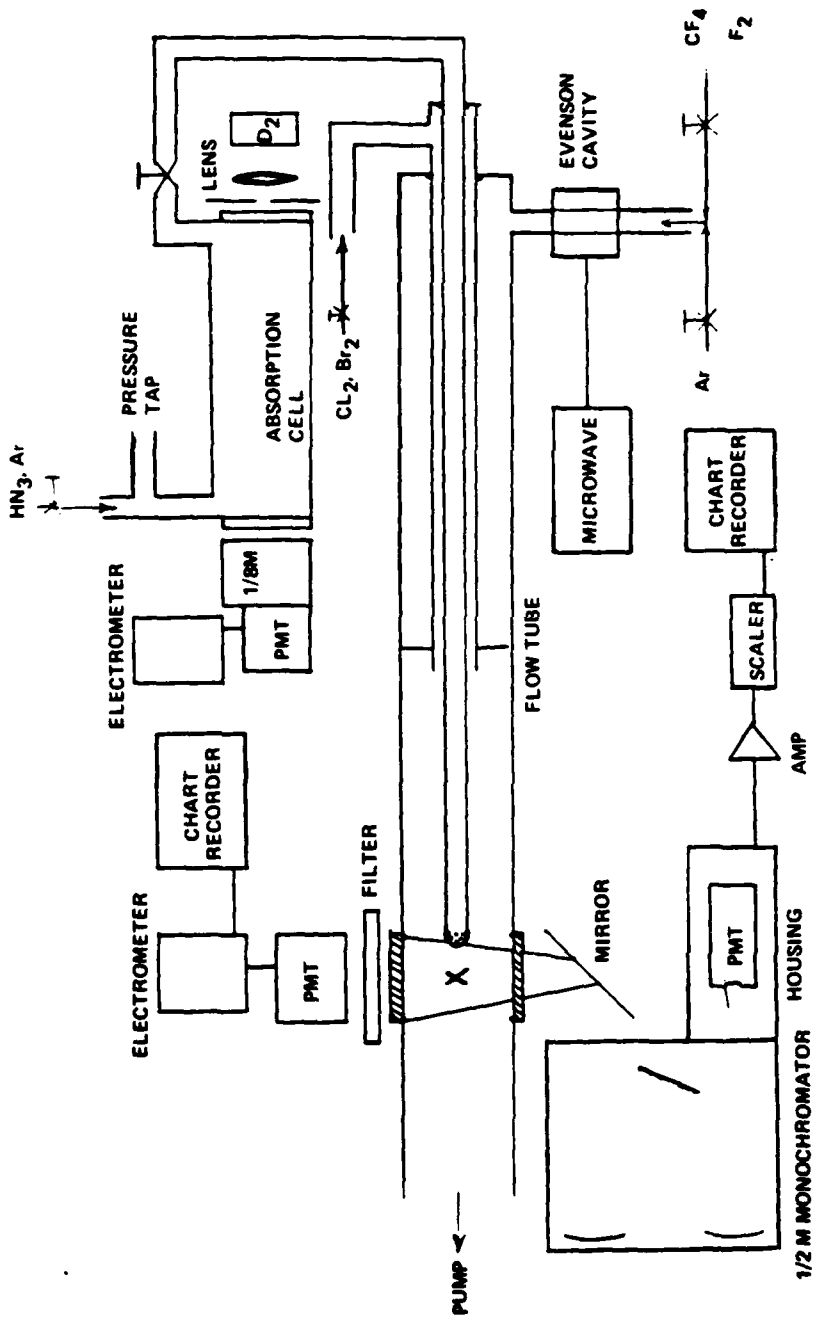

Fig. 2 Schematic of the triply concentric flow tube apparatus.

inner annulus. The reaction of the source gases with F-atoms is known to be rapid, and for the flow velocities of the gases, complete reaction could be obtained prior to the addition of a third reagent in the innermost tube 10 cm further downstream. The reagents of interest in this study which were added to the flow of halogen atoms was HN_3,ClN_3, and HNCO.

Chemiluminescence was viewed at right angles to the direction of flow through fixed windows (CaF_2) attached via viton o-ring seals to the Teflon flow tube reactor. Temporal profiles of the chemiluminescence flame was obtained by movement of the inner slide tube assembly. Visible radiation after reflection by a mirror, as shown in Fig. 1, was passed through a filter, and a 1/2-m (f/8) McKee-Pederson monochromator fitted with a 5 cm square 1200 lines/mm grating blazed at 500 nm. The dispersed emission was detected by a cooled GaAs photomultiplier tube (RCA C31034). The photoelectric pulses were amplified and counted by an SSR model 1110 computer. The count rate after conversion to an analog signal was recorded on a strip chart recorder. Infrared emissions were viewed opposite to the visible emission view port. These emissions, after passage of appropriate filters, was dispersed by a 1/4 meter f/3.2 Jarrell-Ash monochromator, and detected by a liquid nitrogen cooled intrinsic Ge detector system (Applied Detector Technology) having a $D^*(\lambda = 1.1\ \mu m)$ of 2.0×10^{15} cm $Hz^{1/2}$ $watt^{-1}$. The amplified signal was sent directly to a lock-in amplifier (PAR 124A), which was gated by the output of a chopper which was positioned between the reactor flow tube and the monochromator. Photon calibration of the flow tube reactor was accomplished by means of the NO chemiluminescence technique developed by Fontijn et al.[13] for the 500-880 nm region.

The flow rate of all primary gases were monitored by Tylan mass flowmeters calibrated against N_2 flow. Actual flow rates of the gases were obtained by multiplying the flow rate readings by a correction factor supplied by the manufacturer for most of the gases. For those gases not covered by the manufacturer, the correction factor was obtained from a ratio of the heat capacity of N_2 to that of the gas in question. The total pressure in the flow

reactor was monitored by a factory calibrated MKS Baratron capacitance manometer constructed of stainless steel. The partial pressure of each gaseous constituent was calculated in the usual way by

$$P_i = \frac{Q_i}{\Sigma Q_i} P_t \qquad (2)$$

The bottled gases used in this study are presented in Table I, along with the manufacturer and the manufacturer's state purity. The gases were used directly from the storage tank without further purification unless stated otherwise in the text.

Table I. Gas Purity and Manufacturers

Gas on Gas Mixture	Grade and Stated Purity	Manufacturer
F_2	98.0%	Air Products
Cl_2/He	3% Cl_2 in He	Matheson
NO	98%	Matheson
CO_2	Coleman, 99.99%	Matheson
Cl_2	99.5%	Matheson
Ar	99.9995%	Matheson
N_2		Air Products
HCl	Electronic, 99.99%	Matheson
H_2	UHP, 99.999%	Matheson
ClF	- - -	Ozark
HF	99.9%	Matheson

Titration of Fluorine Atoms. Reaction of F-atoms with HCl or Cl_2 is known to be rapid generating HF or ClF, respectively. The reverse reaction of Cl + F_2 is known to be very slow.[14] Titration of the F-atoms was accomplished by the technique of Ganguli and Kaufman[13] in which metered flows of Cl_2 or HCl is added to the F-atom flow. The resulting production of Cl atoms slowly

recombine via a three-body process forming some Cl_2 A-X emission. As the Cl containing reagent is added, this red emission increases quadratically and sharply reaches a plateau when all the F-atoms are consumed. The RCl flow, which corresponds to this sharp endpoint, is the F-atom flow. Hence, the F-atom partial pressure is obtained by Eq. (2). The observed Cl_2 emission intensity at the endpoint remained constant when the slide tube assembly was moved away from the viewing port, implying that surface recombination for Cl atoms was not a significant loss of Cl atoms in this apparatus. With this titration technique, F and Cl atom concentrations were determined, and any mixture could be attained. This technique proved to be a useful tool in analyzing the hybrid chemical reaction discussed in the following subsection.

Unfortunately, addition of Br_2 to the flow stream was non-quantitative due to rapid corrosion of the flowmeter, and uncertainty in maintaining known mixtures of Br_2 in a buffer gas. The F + Br_2 reaction is rapid and mixtures of F and Br atoms were obtained, since the reverse Br + F_2 reaction is also slow.[15]

Generation of HN_3. Gaseous HN_3 was generated on-line for this program since storage of HN_3 in the condensed phase leads to spontaneous detonation. Storage in large tanks, though possible, was not particularly convenient, hence on-line generation was used.

The flow reactor for generating HN_3 is depicted in Fig. 3. A 75% aqueous solution of H_2SO_4 (or D_2SO_4 for making DN_3) was slowly dropped on a bed of solid sodium azide. A buffer gas, generally argon, was passed through the reactor at atmospheric pressure. The buffer gas containing HN_3 and presumably, H_2O, passed through a dry column containing Drierite ($CaCl_2$) and into a fume hood. Under these conditions, infrared spectral scans in the gas showed only those bands associated with HN_3[16], while the water bands were totally absent, implying that the water content must be less than a few percent of the total HN_3 present. A small portion of the flow was directed through a mass flowmeter and a UV absorption cell to monitor the optical

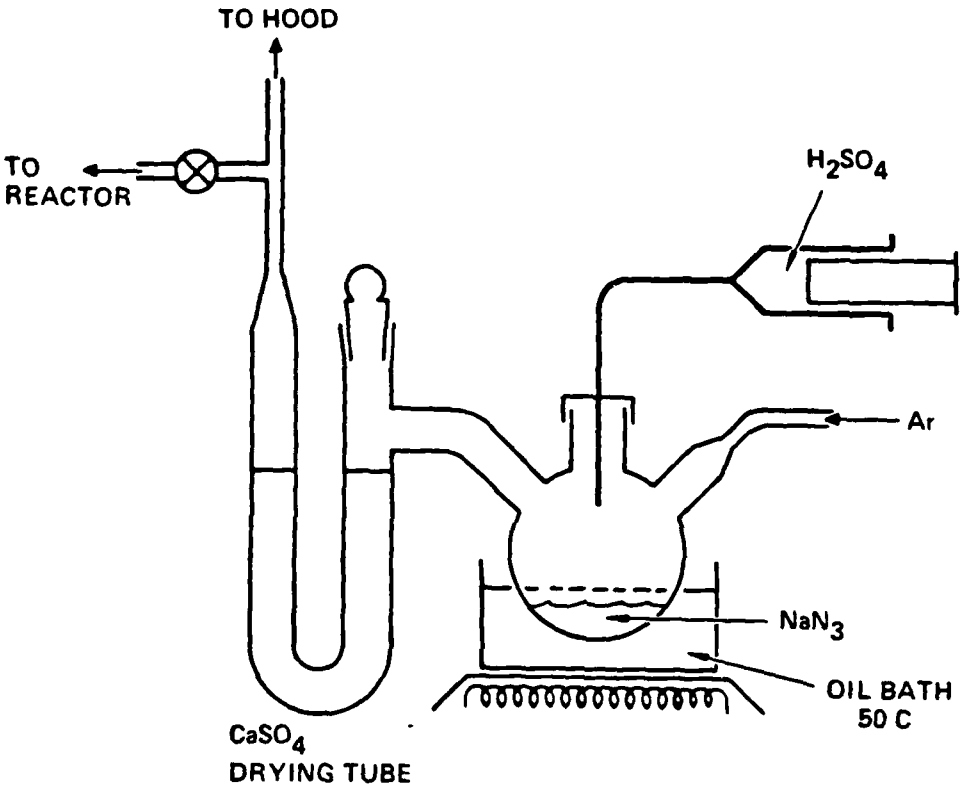

Fig. 3 Schematic of the HN_3 generator.

density of HN_3. The optical density was measured by passing the output from an Oriel D_2 lamp thorugh a narrowband filter at 210 nm, and subsequently through a 5.8 cm long absorption cell. The UV light was dispersed by a 1/8 m Oriel monochromator and detected by a 1P28 photomultiplier tube, whose current was monitored by a Keithly electrometer. The D_2 lamp intensity was purposely kept as low as possible to prevent any significant dissociation of HN_3 in the absorption cell. The total pressure of the absorption cell was monitored by a Validyne inductance manometer. The fraction of HN_3 in the buffer gas flow was calculated from the known extinction coefficient[2] of HN_3 at 210 nm and the total pressure in the cell. Fractions of HN_3 as high as 0.06 were obtained, indicating that the reactor partial pressures were no greater than 45 Torr, which is well below the boiling point pressure for HN_3 at room temperature.[17] The entire reactor, however, was immersed in an oil bath at 323K. A lucite box surrounded the reactor for additional safety.

Generation of ClN_3. Like HN_3, chlorine azide is an unstable species which must be generated on-line in the laboratory. Storage in condense phases in not feasible, since halogen azides often explode upon condensation or evaporation. Hence, an on-line ClN_3 generator was developed for use in the chemiluminescence flow reactor, and in the pulsed photolysis experiment described in Section 3.1.

A diagram of the apparatus constructed for this purpose is shown in Fig. 4. ClN_3 is produced when a stream of Cl_2 heavily diluted in helium (0.1% - 3.0% Cl_2) is passed over solid NaN_3 suspended on glass wool in a pyrex U-tube held under vacuum.[18] Very little ClN_3 is formed unless a drop or two of H_2O is added to the upstream end of the U-tube. More precise means of adding H_2O to the system, such as passing the Cl_2/He over a water reservoir maintained at a known temperature, resulted in yields smaller than those obtained with this rather inexact approach. H_2O impurities are removed from the flow stream by passage of the reactor effluent through a second U-tube containing anhydrous $CaCl_2$ ("Drierite"). ClN_3 concentrations in the effluent stream were measured by observing the UV absorption of this species at

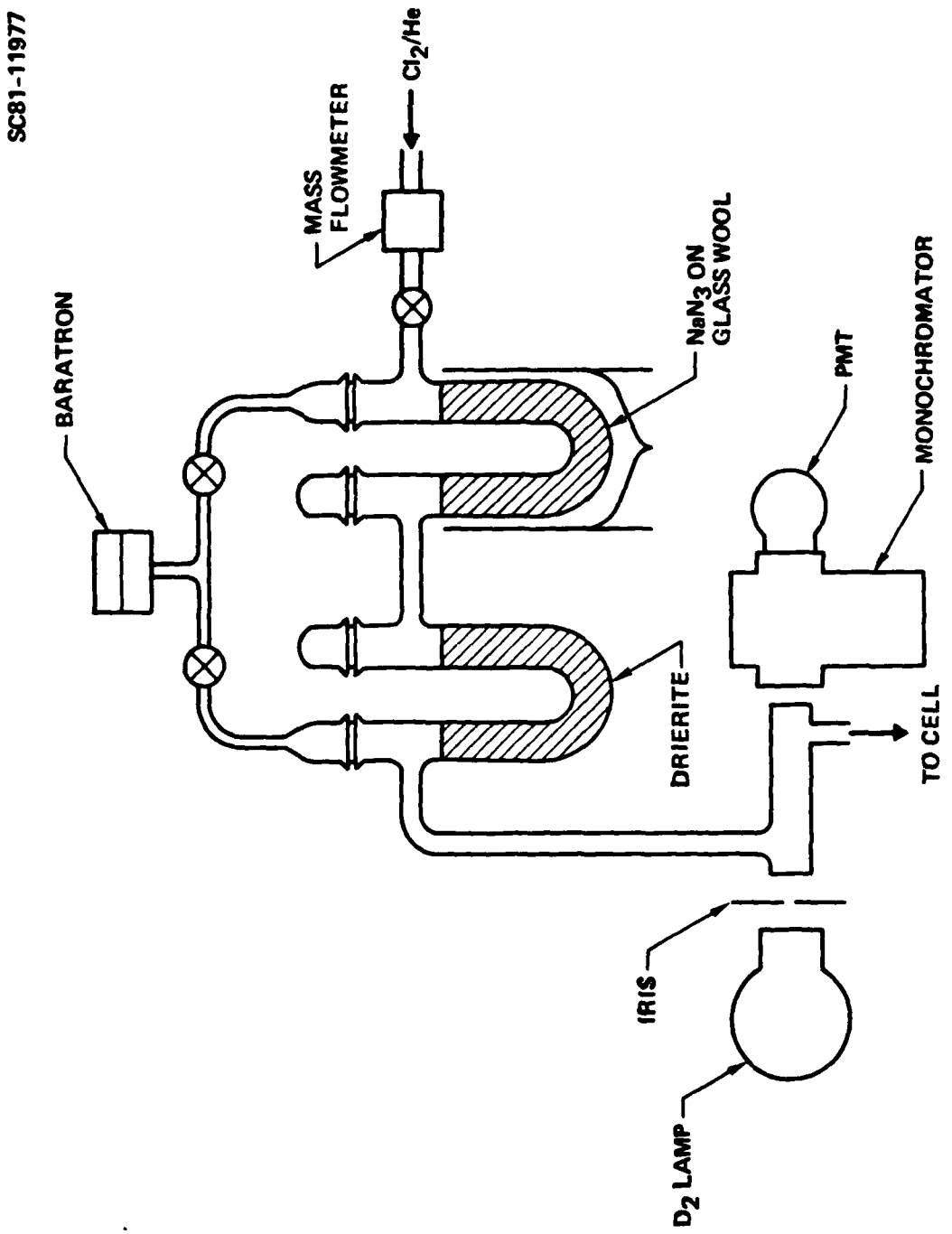

Fig. 4 Schematic of the ClN_3 generator.

0.250 nm. For this purpose, a 10 cm cell equipped with CaF_2 windows was installed on-line in the vacuum system. The extinction coefficient was determined by measurement of known concentrations of ClN_3, and this work is reported in Section 2.2. A D_2 lamp was used as the light source for the absorption monitor. The best runs gave a ClN_3 yield (with respect to the Cl_2 flowrate) of 80% - 100%. Infrared analysis using this same cell indicated that no IR active impurities (e.g., H_2O or HN_3) were present to within the detection limit of the system. Hence, this apparatus proved to be most effective in the generation of ClN_3.

1.2 The F/Cl + HN_3 Flame

Our earliest experiments on azide systems involved studies of the reaction of fluorine atoms with HN_3.[8] The results were consistent with a mechanism in which the initial reaction yields a free N_3 radical, which can subsequently react with another fluorine atom to produce primarily NF* ($^1\Delta$). The NF($^1\Sigma^+$) observed in the flame of the reaction is produced in large measure by a resonant energy pooling process between NF($^1\Delta$) and vibrationally excited HF ($v > 2$).[19] A different situation may exist for the analogous process producing excited NCl. The exothermicity of the Cl + N_3 reaction is more than sufficient for direct production of the $^1\Sigma^+$ state of this molecule. Prior to our experiments, this was, in fact, the only excited singlet state of NCl that had been spectroscopically observed.[6,20]

The heavier nitrogen halide diatomics are more interesting with respect to potential lasing, since relaxation of the optical spin selection rules in these systems results in intrinsically higher gain. Similarly, however, dynamic constraints for the production of excited singlet products by the X + N_3 reactions may also be relaxed. An additional incentive for undertaking studies of the NCl and NBr systems lies in the fact that the initial processes (X + HN_3) may have different efficiencies for the production of N_3 radicals. Recent experiments by Sloan and co-workers have shown that these reactions may be addition-elimination processes rather than direct abstrac-

tions forming HX.[21] Hence, generation of N_3 may compete with formation of HNX fragments, the proportion depending on the degree of energy randomization in the HXN_3 complex. Different systems may therefore have different efficiencies for formation of N_3.

The experiments involved temporal profiles and relative densities of excited species produced by these reactions as a function of the reagent concentrations. The results of a vibrational analysis of the NCl emission spectra in the visible and near-infrared are discussed in a subsequent section. The results are published in reference 22. The fundamental conclusions drawn from the data are as follows:

a. The most efficient source of excited NCl ($^1\Delta$, $^1\Sigma^+$) is the reaction of a mixture of fluorine and chlorine atoms with HN_3. The F atoms actively participate in the reaction, which proceeds via the following "hybrid" mechanism:

$$F + HN_3 \rightarrow HF + N_3 \quad (3)$$

$$Cl + N_3 \rightarrow NCl\ (^1\Delta,\ ^1\Sigma^+) + N_2 \quad (4)$$

b. The efficiency of the hybrid mechanism results from an optimum combination of rates. Rate constants for competitive processes involving Cl and F atoms were observed to have the following values:

$$k\ (F + HN_3) > 1 \times 10^{-11}\ cm^3\ molecule^{-1}\ s^{-1} \quad (5)$$

$$k\ (Cl + HN_3) < 1 \times 10^{-12}\ cm^3\ molecule^{-1}\ s^{-1} \quad (6)$$

$$k\ (F + N_3) \approx 2 \times 10^{-11}\ cm^3\ molecule^{-1}\ s^{-1} \quad (7)$$

$$k\ (Cl + HN_3) \approx 1 \times 10^{-11}\ cm^3\ molecule^{-1}\ s^{-1} \quad (8)$$

The last value, reported for comparison, was obtained by Jourdain and co-workers.[6]

c. The intensities of both the $^1\Delta$ and $^1\Sigma^+$ states of NCl rise linearly with the HN_3 flowrate, suggesting that both may be produced directly by the Cl + N_3 reaction (in contrast to the NF case).

1.3 F/Br + HN_3

Addition of molecular bromine in place of molecular chlorine also produced a brilliant red flame consisting of the b-X transition of NBr. Again, approximately 90% of the emission was from the $\Delta v = 0$ transitions. A description of these vibrational bands and their analysis, and rotationally resolved spectra and their analysis is given in subsection 1.6. As in the case with Cl_2 addition, a sharp peak in the NBr 0-0 band intensity was observed as the bromine was added to the flow. In addition, the N_2 first positive emission grew weaker as bromine was added. Qualitatively, it appeared that the N_2 B-A emission was not quenched as rapidly as was the case with Cl_2 addition. We interpret this result as a slower rate constant for the Br + N_3 reaction relative to the Cl + N_3 reaction. Infrared emissions were also observed and identified as the $a'^1\Delta - X^3\Sigma^-$ emission for NBr analagous to those of NCl. Since the chemiluminescence behavior is similar to that of the F/Cl + HN_3 reaction, we suspect that the NBr ($b^1\Sigma^+$) production is the result of the hybrid reaction

$$F + HN_3 \rightarrow HF + N_3 \quad (9)$$

$$Br + N_3 \rightarrow NBr\ (a^1\Delta,\ b^1\Sigma^+) + N_2 \quad (10)$$

The emission intensity for NBr b-X transition was more intense than those for the NCl b-X emission, indicating that perhaps the radiative lifetime of NBr b state is shorter than that for NCl b state, and therefore competitive with quenching processes taking place in the flame.

1.4 The F+ ClN_3 Flame

The reaction of fluorine atoms with ClN_3 is of some interest since, in contrast to the F + HN_3 case, no resonant energy pooling mechanism exists for the production of NF ($b^1\Sigma^+$). A small discharge-flow apparatus was constructed from quartz to study this reaction. Fluorine atoms were produced by microwave discharge through CF_4. For conditions under which the ClN_3 yield from the generator was high, the emission spectrum produced by the reaction consisted primarily of NF($^1\Delta$), NF($^1\Sigma^+$), and NCl($^1\Sigma^+$) features with the NF($^1\Delta$) band being by far the most intense. The excited NCl present in the flame was produced by the Cl + ClN_3 reaction, which has been previously studied by Clark and Clyne[6]. Chlorine atoms were generated by the reaction of F atoms with residual Cl_2 passed through the generator. The excited NF was most likely produced as follows:

$$F + ClN_3 \rightarrow ClF + N_3 \qquad (11)$$

$$F + N_3 \rightarrow NF^* + N_2 \qquad (12)$$

Emission from NF($^1\Sigma^+$), though considerably less intense than that from NF($^1\Delta$), was still evident even when no HF overtone emission was present in the spectrum. Results of measurements of the NF and NCl intensities vs the ClN_3 concentration are shown in Fig. 5. Clearly, the NF($^1\Sigma^+$) signal does not rise faster than the NF($^1\Delta$) signal, indicating that a pooling process (e.g., NF($^1\Delta$) + NCl($^1\Delta$)) is not responsible for the production of the $^1\Sigma^+$ state. Hence, we conclude that a small fraction of the F + N_3 collisions result in direct production of NF($^1\Sigma^+$), setting a lower limit on the exothermicity of the process: $\Delta H > -54$ kcal/mole.

Some experiments have been performed on the Cl + ClN_3 system. The most significant observation is that the peak intensity of the NCl($^1\Sigma^+$) emission produced is more than the order of magnitude less than that produced by the F/Cl + HN_3 system for comparable reagent concentration.

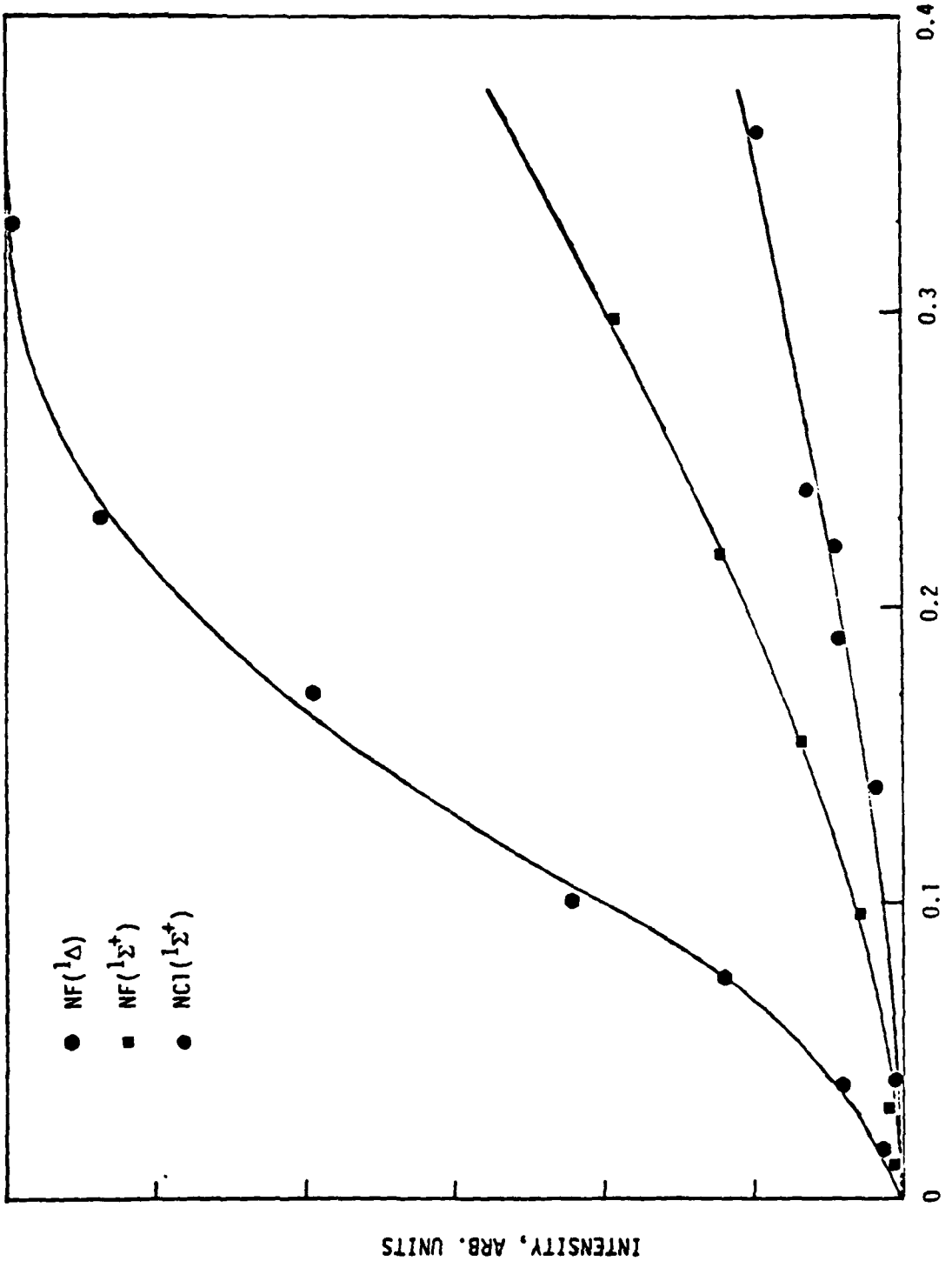

Fig. 5 Relative intensities of NF($a^1\Delta$), NF($b^1\Sigma^+$) produced in the F + ClN_3 reaction vs the initial ClN_3 pressure.

1.5 F + HNCO

Hydrogen isocyanate is isoelectronic with HN_3, but the reaction thermodynamics are much different owing to the increased bond strengths of both the H-NCO bond in HNCO and the N-CO bond strength in the isocyanate radical. Hence, the analogous F-atom reactions have the following exothermicities,

$$F + NHCO \rightarrow HF + NCO \qquad \Delta E = 23 \text{ kcal/mole} \qquad (13)$$

$$F + NCO \rightarrow NF + CO \qquad \Delta E = 26 \text{ kcal/mole} \qquad (14)$$

Only the v=2 level of HF can be populated by reaction (13), and only NF in its $X^3\Sigma^-$ ground state can be generated by reaction (14). If spin is an important constraint on reaction (14), then the reaction is slow and consequently the concentration of NCO radicals can attain significant proportions in the flow.

Gaseous HNCO was prepared by the method of Asby and Werner.[23] Briefly, a saturated solution of KOCN was slowly dropped by gravity under vacuum into a reaction vessel containing 100% phosphoric acid agitated by a magnetic stirrer. The entire reaction vessel was immersed in an ice water bath. The evolved gases were pumped out of the reaction chamber and passed through a U-tube trap maintained at 173K. After the reaction was completed, the condensed material in the trap was gently warmed and transferred to an IR absorption cell. Spectroscopic analysis of the trapped gases clearly identified the presence of HNCO, but the possible impurity bands associated with HCN, NH_3, or CO_2 were absent. The HNCO was carried from the U-trap vessel to the central tube of the chemiluminescence flow tube apparatus by a buffer gas, N_2.

Adding HNCO to the stream of F-atoms generated a bright blue flame. The UV and visible spectrum of this chemiluminescence flame is shown in Fig. 6. This spectra is the only information obtained in the F + HNCO flame study, and therefore represents only a preliminary investigation; hence, much

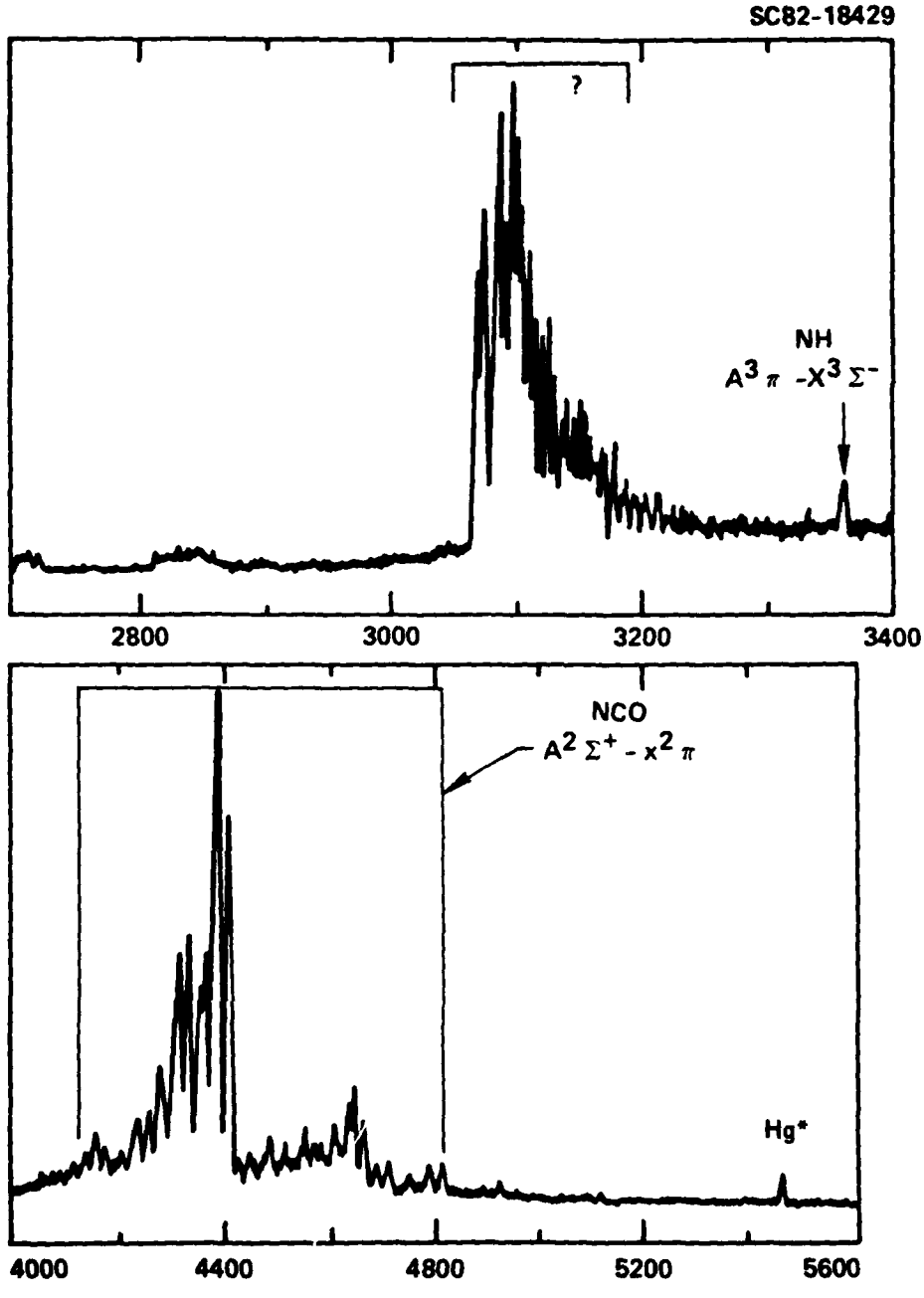

Fig. 6 UV-visible spectrum of the F + HNCO flame.

of the following discussion is speculative. The blue emission is the $A^2\Sigma^+$ - $X^2\Pi$ bands of NCO. The intense UV bands, which are red-degraded and have an apparent band head at 310 nm, remain unidentified. They do not appear to be associated with the $B^2\Pi$ - $X^2\Pi$ system of NCO which occurs in the 260-320 nm region, and they are definietly not the $c^1\Pi$ - $a^1\Delta$ bands of NH. The $A^3\Pi$ - $X^3\Sigma^-$ emission band of NH, however, is clearly seen at 336 nm. The weak UV band at 285 nm could be part of the B-X emission of NCO.

Clearly, from the exothermicities of reaction (13) and (14), energy pooling processes must account for the observed fluorescense. The second order reaction

$$NCO + NCO \rightarrow N_2 + 2CO \qquad (15)$$

does not have sufficient energy to populate the $A^3\Sigma^+$ state of N_2, but if the two NCO reagents between them have 30 kcal/mole of energy which could come from reaction (13), $N_2(A)$ could be formed, and the observed emissions could be explained. Collision of $N_2(A)$ with NCO can easily populate both the band A and B states of NCO. The formation of NH ($A^3\Pi$), however, requires a two step reaction sequence as follows:

$$N_2\ (A) + HNCO \rightarrow NH\ (X) + CO + N_2 \qquad (16)$$

$$N_2\ (A) + NH\ (X) \rightarrow N_2\ (^1\Sigma^+) + NH\ (A) \qquad (17)$$

Unfortunately, we did not have the means of calibrating the collection efficiency of the spectrometer-detector system in the blue region of the spectrum, and therefore we have not been able to assess the photon yield associated with the A-X emission of NCO relative to the HNCO reagent concentration.

Not shown in Fig. 6 is the spectrum from 560-900 nm. There was no emission in this region. Hence, emissions from CN were not observed. Moreover, the HF $v = 3 \rightarrow v = 0$ band and the NF $a^1\Delta \rightarrow x^3\Sigma$ 0-0 bands are also

missing in accord with the stated energetic associated with reaction (13) and (14).

Addition of molecular chlorine in the inner annulus of the flow tube resulted in the disappearance of the blue emission. The presence of Cl atom in the flow permits the following spin allowed reaction,

$$Cl + NCO \rightarrow NCl\ (a^1\Delta) + CO \qquad (18)$$

Hence, a search for the NCl $a^1\Delta - X^3\Sigma^-$ emission at 1.07μm was conducted, but without success. The HF $v = 2 \rightarrow v = 0$ bands were observed at ~1.3μm as would be expected by reaction (13). The occurrence of reaction (18) is still an open question, since care must be used in adding the molecular chlorine to the flow, and time did not permit a detailed optimization of the flow to find the NCl $a^1\Delta$ state.

1.6 Analysis of the Singlet-Triplet Intercombination Bands of NCl and NBr

Relative to a number of isoelectronic molecules comprised of atoms of groups VA, VIA, and VIIA, very little information exists concerning the spectroscopy of the ground and lower lying excited states of nitrogen halide diatomics. No absorption data have been reported, presumably because of the lability of the ground state species. An exception is the tentative assignment by Briggs and Norrish of bands observed near 240 nm to the $X^3\Sigma^- \rightarrow A^3\pi$ transition in NCl.[24] These data, obtained from the flash photolysis of NCl_3, have not been reproduced. The majority of spectroscopic information concerning NCl and NBr has been obtained from emission studies of discharges through N_2-halogen gas mixtures.[20,25,26] Prior to our work in the area, only the $b^1\Sigma^+ \rightarrow X^3\Sigma^-$ transitions in the visible had been identified. Work by Clyne an co-workers on ClN_3 reactions produced an extensive spectrum of this transition in NCl, but emission from the lower lying $a^1\Delta$ state was not found.[6,7]

Our flow tube studies of halogen atom-HN_3 reactions offer an excellent opportunity for studying the spectroscopy of NX molecules, since these

systems produce very bright localized NX flames. Spectra of these flames were recorded using two different detection systems. Visible emissions were dispersed by a 0.5 m McKee-Pederson monochromator prior to being detected by a photon counting system consisting of a cooled GaAs photomultiplier tube and a PAR amplifier discriminator and scaler. Infrared emissions were observed using a 0.25 m Jarrell-Ash monochromator and a liquid N_2 cooled intrinsic germanium detector, which has high sensitivity in the 1 μm regime. Spectra were recorded for flames producing excited NCl and NBr. The details of these experiments and the results obtained are published in reference 27. The main results are as follows:

a. Emissions from the $a^1\Delta$ states of NCl and NBr were observed for the first time. The 0,0 bands of these transitions occur at 1.077 and 1.078 μm, respectively. Observation of transitions from higher v' levels permitted calculation of vibrational constants for these states. These calculations indicated good agreement with the known constants of the respective ground states, affirming our assignment of the bands to $a^1\Delta \rightarrow X^3\Sigma^-$ transitions.

b. The azide flames produced the most extensive spectra of the visible $b^1\Sigma^+ \rightarrow X^3\Sigma^-$ transitions of NCl and NBr yet recorded, including 40 bands of this transition in NCl and 28 in NBr. Many of these bands have not been previously observed, in particular, for the NBr case. Molecular constants calculated from the data agree well with values previously reported from high resolution studies.

c. The $b^1\Sigma^+ \rightarrow X^3\Sigma^-$ transition in NBr exhibits a double progression which we believe results from Hund's case c splitting of the ground $X^3\Sigma^-$ state into $\Omega = 0^+$ and $\Omega = 1^\pm$ components. Each of the NBr bands observed exhibits two heads, the more intense head

corresponding to a transition to the $\Omega = 0^+$ state. This progression corresponds to bands reported from previous emission studies.[26] The second progression corresponds to transitions to the $\Omega = 1^{\pm}$ states, and is red-shifted from the more intense progression by about 40 cm^{-1}. These transitions have been cited as "missing" in previous studies of the NBr spectrum.

d. Values of the relative Franck-Condon factors calculated from observed intensity relationships among the bands of the $b^1\Delta^+ \rightarrow X^3\Sigma^+$ transitions do not agree well with previously calculated values published in the literature.[27] Similarly, the relative intensities of transitions to the $\Omega = 0^+$ and $\Omega = 1^{\pm}$ states in NBr do not agree with calculations based on values of rotational and spin-rotational constants in the literature.[26]

Molecular constants for the $a^1\Delta$ and $b^1\Sigma^+$ states for both NCl and NBr are given in Table II. Franck-Condon factors for the b-x transition in NBr is given in Table III.

Table II. Molecular Constants for the Three Low Lying States of NCl and NBr.

	NCl			NBr		
	$X^3\Sigma^a$	$a^1\Delta b$	$b^1\Sigma^{+a}$	$X^3\Sigma^c$	$a^1\Delta b$	$b^1\Sigma^{+c}$
Te	0	9240[a]	14984.6[b]	0	9246[a,c]	14787.3[d]
ωe	827	904	935.6	691.1	763	785.5
ωeXe	5.1	4.7	5.4	4.71	2.4	4.35
Bo	0.6468	---	0.6828	.4455	---	.4712
Do	1.78×10^{-6}	---	1.65×10^{-6}	---	---	---
λ	1.776			12.17		
γ	0.0071			-0.0599		

a. Reference 20
b. Reference 27
c. This work

Table III. Franck-Condon Factors for the b-x Transistor in NBr.

v' \ v"	0	1	2	3	4
0	0.843 (0.606)[a]	0.143 (0.288)	0.014 (0.083)		
1	0.137 (0.317)	0.180 (0.148)	0.103 (0.303)	0.016	
2	0.020 (0.069)	0.182 (0.377)	0.024 (0.076)	0.071	0.016

a. Values in parenthesis refer to Franck-Condon factors calculated in Reference 28.

Since the intensity of the 0-0 band in the b-X transition in NBr from the F/Br + HN_3 flame is so intense, we were able to rotationally resolve the weaker red-shifted band, and verify that it contained the "missing" ^{O}P and ^{Q}R branches. The details of the spectra and its analysis are presented in manuscript form in Appendix A. The analysis of all four branches (^{Q}R, ^{O}P, ^{S}R and ^{Q}P) yielded accurate values for the spin-spin, and spin-rotation constants, which are present with the B_0 values in Table II.

2. UV - Vacuum UV Absorption of the Halogen Azides

A very limited amount of information exists regarding the ultraviolet spectra of halogen azide molecules. Recently, Dehnicke and Ruschke reported UV spectra above the quartz limit (200 nm) for ClN_3, BrN_3, and IN_3 in liquid solutions.[29] The spectrum of ClN_3 in the gas phase was reported by Clark and Clyne,[7] and the FN_3 spectrum has been studied by Haller[16] and in our own laboratory.[12] As is the case for other covalently bound azides, however, it is probable that the strongest absorptions in these molecules occur in the vacuum UV. Hence, our goal in these experiments is the measurement of accurate spectra at wavelengths down to ~150 nm to aid in our understanding of the nature of excited fragments produced by photolysis in this regime.

2.1 The UV-Vacuum UV Apparatus

The apparatus constructed for the measurement of UV absorption spectra is shown in Fig. 7. It consists of a 0.3 m McPherson monochromator equipped with MgF_2 coated optics and a grating blazed at 200 nm, a vacuum UV source lamp (McPherson 630, powered by a Universal Voltronics power supply) which can be used with a variety of gases, a 10 cm absorption cell equipped with CaF_2 windows, and a CsTe photomultiplier tube (EMI 626315) sensitive in the 150 nm - 300 nm region. The apparatus is configured such that UV light from the source is dispersed by the monochromator prior to entering the absorption cell. Hence, emission from excited fragments produced by photolysis at particular wavelengths may be observed. The absorption cell is equipped with a side window for the purpose of detecting such emission.

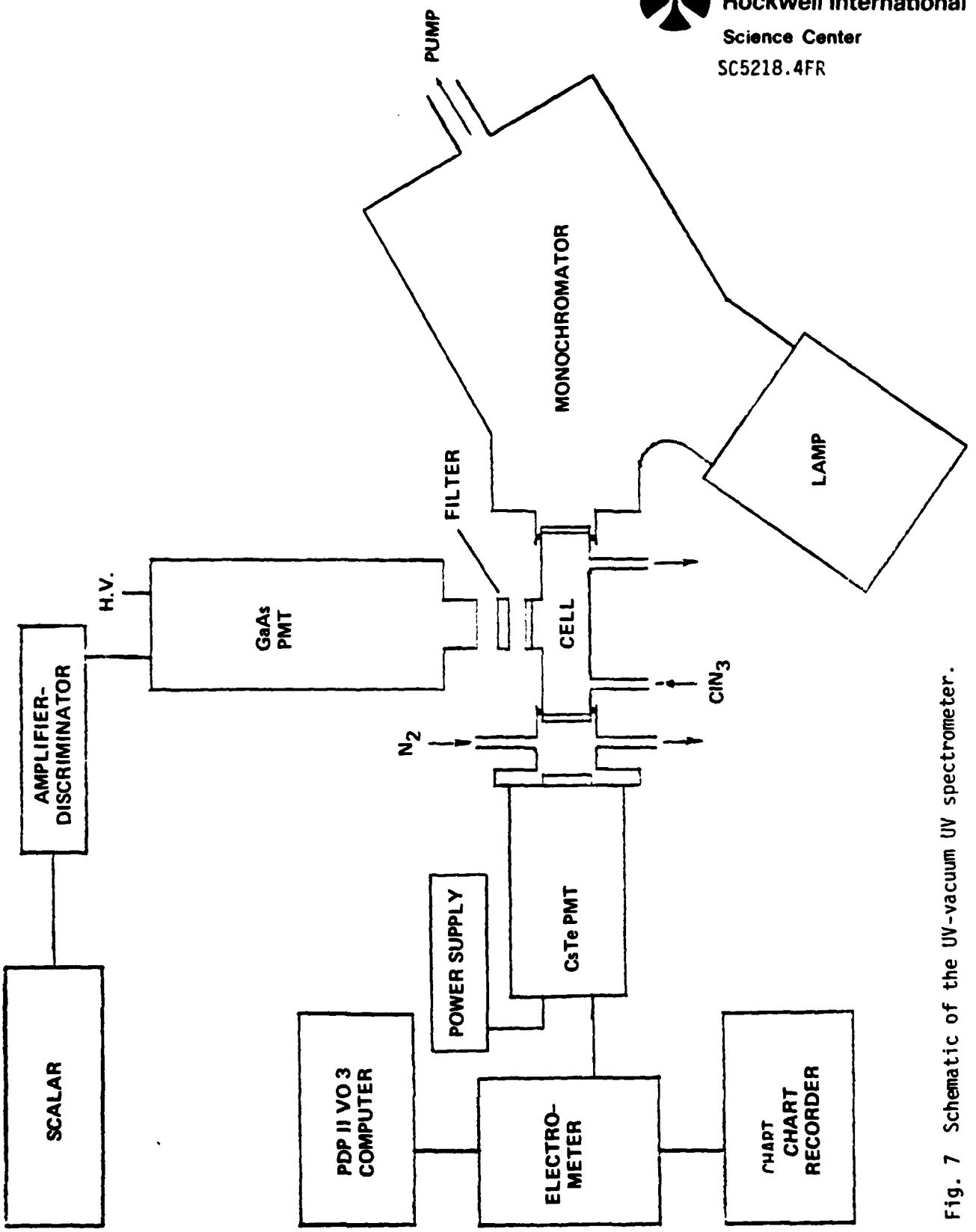

Fig. 7 Schematic of the UV-vacuum UV spectrometer.

The majority of the absorption spectra measured to date have been obtained using argon in the source lamp. The argon discharge was found to produce a relatively smooth continuum extending down to ~170 nm, where a large singularity was observed. This feature does not correlate with known features of discharged argon, and may be caused by an impurity in the gas. The response of the CsTe PMT was recorded by an electrometer prior to being stored in a small laboratory computer (DEC 11V03), which enabled the baseline of the lamp output to be automatically subtracted from spectra recorded with the halogen azide in the cell.

2.2 UV-Vacuum UV Absorption of ClN_3

Our experiments began by measurement of the absorption spectrum of ClN_3 in the UV-vacuum UV region. The spectrum exhibits three distinct regions of absorption, as shown in Fig. 8. The two longer wavelength features (λ_{max} = 205 nm and 250 nm) are in good agreement with the spectrum above the quartz limit reported by Clark and Clyne,[7] and are qualitatively similar to features found in the spectra of other simple azides, such as HN_3 (also shown in the figure). We note, however, that unlike the spectra of HN_3 or HNCO, the ClN_3 spectrum exhibits no structure in these absorption regions, suggesting that the upper states of the transitions may be repulsive. Clearer differences between the transitions in ClN_3 and HN_3 or HNCO were evident in the photofragment and their internal energy distribution. These experiments are described in detail in Reference 30 and summarized in Section 3.2.

A GaAs red-sensitive photomultplier tube was attached to the absorption cell at right angles to the absorption path in the hopes of observing electronically excited photodissociated products. The PMT was fitted with a Corning red pass filter such that wavelengths only greater than 600 nm were passed. When the argon lamp was off and no gases flowed through the absorption cell, we obtained the normal dark photon count rate. Addition of flowing ClN_3/He to the absorption cell resulted in an increased count rate. Just as the valve opened, a burst of counts was observed with a rapid decline to count

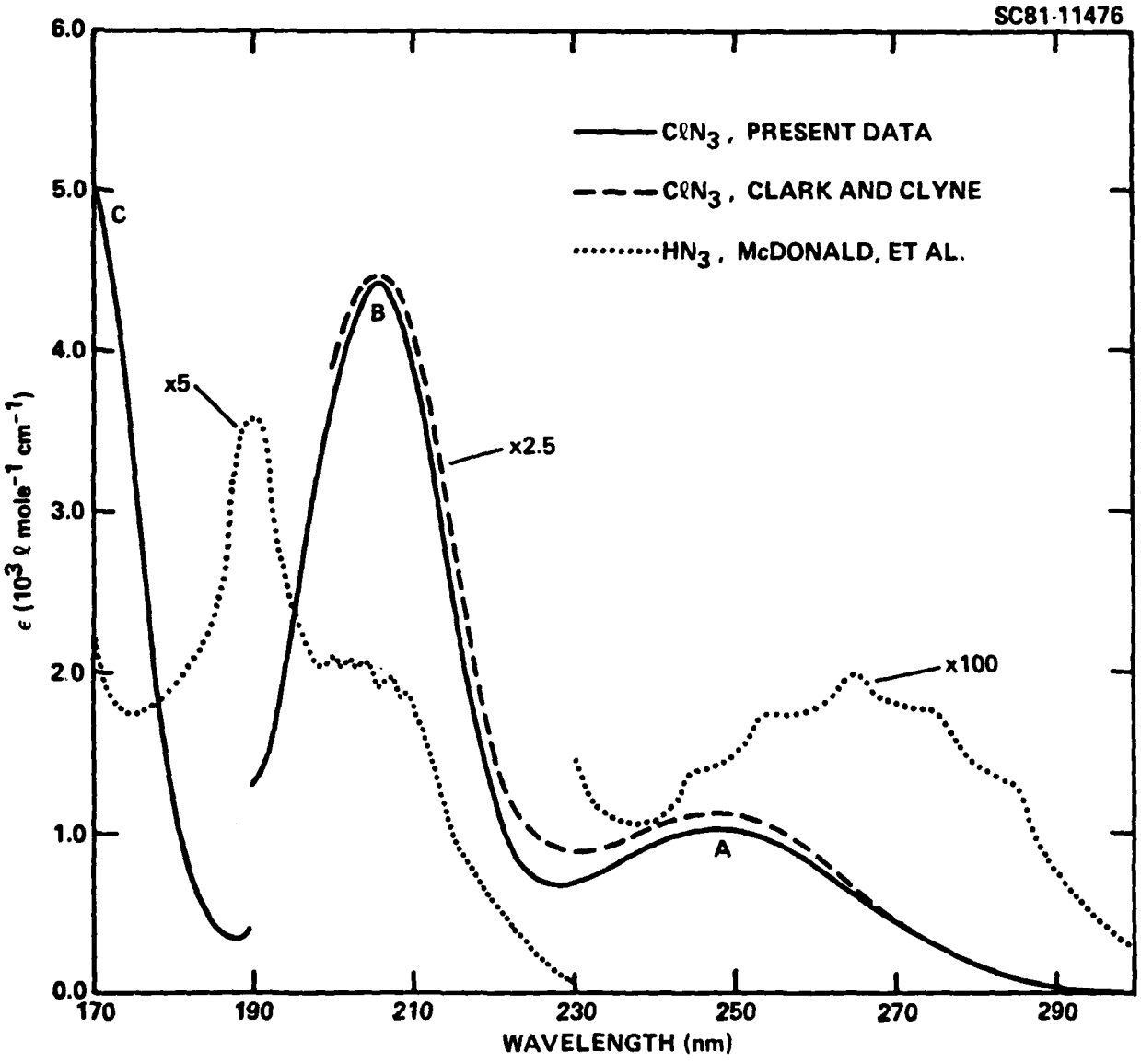

Fig. 8 Absorption spectrum of ClN_3 and HN_3.

rates in excess of the background count rate. One explanation of the observed increased counts when the ClN_3 was initially introduced to the absorption cell is shock formation of Cl atoms and N_3 owing to the weak ClN_3 bond. The red emission can be due to two possibilites, including Cl-atom reaction with N_3 producing NCl ($b^1\Sigma^+$) or from N_3 + N_3 collisions producing the N_2 first positive emissions. When the argon lamp was ignited and the wavelength selected to ClN_3 absorption regions, the red emission rate in the absorption cell increased. These count rates, however, were relatively weak, rendering spectroscopic analysis unfeasible. Since the pulsed photolysis method of analyzing the spectral components was possible, the effort was therefore channeled into the pulsed laser photolysis experiments described in the following section.

3. Time-Resolved, Pulsed Photolysis Studies

3.1 Experimental Details

The basic experimental apparatus which is depicted in Fig. 9 consists of a pulsed excimer laser source, a fluorescence cell, a gas handling system and a fluorescence detection system with associated signal processing and data storage. The photolysis source for these experiments was either a Tachisto TAC II or a Lambda Physik EMG101, which operates on one of three wavelengths, 193, 249, or 308 nm, corresponding to the lasant AF, KrF, or XeCl, respectively. The output power of the laser was monitored by directing a small portion of the output beam onto the surface of a pyrolectric detector (Molectron), whose time-dependent response was captured by a Biomation 610B transient recorder, and subsequently displayed on one channel of a dual beam oscilloscope. The response of the pyrolectric detector was integrated by a PAR CW-1 boxcar integrator. The integrated signal strength was calibrated against the total laser pulse energy measured with a Scientech power/energy meter.

Two T-shaped fluorescence cells were used in the study fitted with CaF_2 windows for the transmission of the laser beam and observation of the

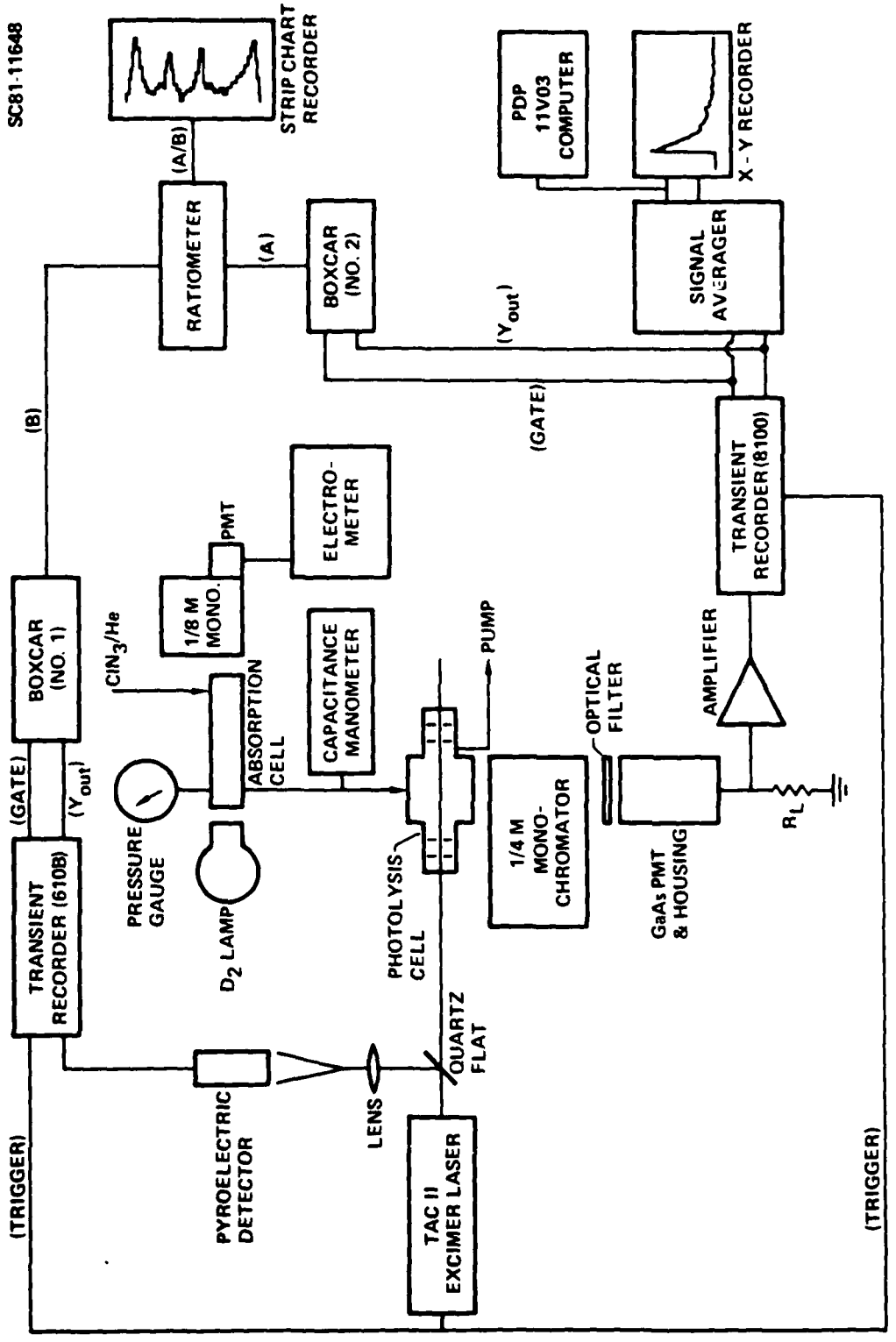

Fig. 9 Schematic of the pulsed photolysis apparatus.

resultant fluorsescence. For the ClN_3 photolysis and NCl decay studies, the cell was fabricated from a Teflon block. The windows for the transmission of the laser beam were extended ~5cm from the cell wall by tubes containing a series of buffers, which effectively reduced interference from spurious window fluorescence. The second cell used for the halogen atom reactions with HN_3 was constructed from a stainless steel block. In this case, however, all windows were directly attached to the cell walls. The light baffles were not required when observing infrared signals.

Emissions produced within the fluorescence cell were monitored in a direction perpendicular to the axis of the laser beam. The UV and visible emissions were dispersed by a 1/4 m monochronator (Jarrell-Ash) equipped with a variable speed drive. The monochromator was calibrated with output of a low pressured Hg lamp. Light emitted in the UV-visible region was detected with a thermoelectrically cooled GaAs photomultiplier tube (RCA C31034) sensitive from 200-880 nm. Infrared emission after passage through selected narrow banded filters were detected by either an LN2 cooled InSb element (3 mm dia.) or by a GaAs element (3x5 mm^2). The output from the detector element was sent to a specifically designed preamp for that element.

Two kinds of experiments were performed with the pulsed photolysis apparatus. Time resolved emission spectra were obtained by slowly scanning the monochromator as the laser was pulsed at 1 Hz. The time-dependent response of the GaAs PMT was amplified (HP 465-A) and digitized by a Biomation 8100 transient recorder. The pulsed emission signal was displayed on the second channel of the dual beam scope. The intensity of the light emitted within a given time interval after the laser pulse was recorded by integrating that portion of the time varying signal with a second PAR CW-1 boxcar integrator equipped with a variable gate width and delay capabilities. The response of the boxcar vs. the wavelength transmitted by the monochromator was recorded on a strip chart recorder. The intensity of the emission signal was normalized to the laser power on a pulse-to-pulse basis by monitoring the ratios of the signals from boxcar #2 (the emission signal) to boxcar #1 (the

laser signal) using the ratiometer portion of a PAR 5204 lock-in amplifier. The overall response of this data collection system was ~0.5 μs for a 50 Ω load on the PMT output.

The second experiment was directed toward measuring the decay kinetics of excited species produced directly in the photolysis, or as a result of a subsequent chemical reaction. For this purpose, the digitized time profiles of the emission signals stored on the transistent digitizer were summed by a Northern Scientific 570 signal averager. The output of the signal average was sent either to a HP X-Y plotter or to a PDP 11V03 microcomputer for data storage and subesequent analysis. The limiting time response was 0.5 μs for UV and visible emission, 1.0 μs for the infrared emission detected by the InSb detector system, and 0.2 μs for the GeAs detector system.

The gas handling system, azide generators and flow monitoring equipment were described earlier in Section 1.1. Total pressure in the photolysis cell were monitored with an MKS Baration capacitance meter. Percentages of ClN_3 or HN_3 from the generator was determined in a manner also described in the aforementioned section. The gases used, including their stated manufacturer purity, are given in Table I.

All gases, except ClF and HF were used without further purification. Chlorine monofluoride was subjected to a series of freeze pump-thaw cycles at 77K, passed through a trap at 131K, and collected again at 77K. Hydrogen fluoride was mixed with F_2 at high pressure and heated for several hours. The F_2 was pumped off and the dried HF was stored in a passivated stainless steel container. This procedure for drying HF is known to reduce H_2O to less than 1 ppm.[30]

3.2 Photochemistry of ClN_3

Chlorine azide was photolyzed using laser sources at 193 nm and 249 nm. In contrast to the situation with HN_3, spin allowed production of both singlet and triplet photofragments is possible at both of these wavelengths as follows:

$$ClN_3 \xrightarrow{h\nu\ laser} \begin{cases} NCl^* (^1\Delta, ^1\Sigma^+, \ldots) + N_2 (^1\Sigma_g^+) \\ NCl (^3\Sigma^-) + N_2^* (A^3\Sigma_u^+) \end{cases} \quad (19)$$

Emission in both the UV and visible regions was found for photolysis at either 249 nm or 193 nm. In fact, the primary difference between results obtained in these two cases is the substantially reduced intensity for KrF photolysis. The magnitude of this intensity reduction relative to ArF photolysis is much greater than expected on the basis of the extinction coefficients at the two wavelengths (see Fig. 8) and argues for a smaller quantum yield at 249 nm. The details of this experiment including the data, its analysis, and the resulting conclusions are given in reference 31. The following is a brief summary of observations and conclusions.

Ultraviolet emission produced by the 193 nm photolysis consisted primarily of a series of bands from 280 nm to 380 nm. These features were readily identified as $C(^3\pi_g) \rightarrow B(^3\pi_g)$ emissions in N_2. The temporal profile of these features exhibited an unresolvable rise (τ_{rise}<500 ns) and a decay time of ~5 μsec. The N_2 emission intensity was found to have a quadratic dependence on the laser energy. This behavior indicates that the emitters were not produced by the direct fragmentation of ClN_3. Although a second order energy dependence would also result from a direct two photon absorption process, the decay time of the N_2 emission argues against such a mechanism. The 5μsec decay time is much longer than the radiative lifetime of this species, and suggests a collisional formation process. The most likely such process is energy pooling between two $N_2(A^3\Sigma_u^+)$ metastable molecules:[32]

$$N_2(A^3\Sigma_u^+) + N_2(A^3\Sigma_u^+) \rightarrow N_2(C^3\Sigma_u^+) = N_2(X^3\Sigma_g^+) \quad . \quad (20)$$

N_2 $(C^3\Sigma_u)$ emission produced in this fashion would exhibit a quadratic energy dependence if $N_2(A^3\Sigma_u^+)$ metastables were produced directly by the ClN_3 photolysis. In view of the forbidden nature of the N_2 A→X transition, emis-

sion from this excited species would not be observable in the spectrum recorded from our pulsed experiments. The presence of $N_2(A^3\Sigma_u^+)$ metastables subsequent to the laser pulse was verified however, by addition of NO to the system. Nitrogen metastables are rapidly quenched by NO, resulting in NO γ-band emission between 200 nm and 300 nm.[11] Very intense NO γ emission was found in the UV spectrum in this case. The time decay of the NO emission was found to agree well with published values for the rate constant of the $N_2(A^3\Sigma_u^+)$ - NO energy transfer process,[32] and the NO emission intensty was linear in the laser energy as expected.

The temporal profile of the visible emission exhibits two distinct components, a fast decay with a time constant on the order of a few hundred μsec. The intensity of both components was found to vary linearly with the laser power, suggesting that the emitters are directly produced photofragments. At the shortest time obtained, corresponding to a delay of 2 μsec and a boxcar gate width of 1 μsec, the spectrum is dominated by a rapidly decaying component. The spectrum shows five distinct regions of emission from λ = 500 nm to λ = 700 nm. These features collapse to a single sharp peak near 665 nm at long delay times, corresponding to emission in the slowly decaying component. This single feature is easily identified as the 0,0 band of the NCl $b(^3\Sigma^+) \rightarrow X(^3\Sigma^-)$ transition. The wavelengths of the five broader emission regions agree will with the expected positions of the $\Delta v = 0$, $\Delta v = 1$, $\Delta v = 2$, $\Delta v = 3$, and $\Delta v = 4$ sequences of this transition, corresponding to emission from vibrational levels as high as $v' = 12$. Hence, the data indicates that NCl $(b^1\Sigma^+)$ is produced with considrable vibrational excitation, and that the rapidly decaying component in Fig. 2 corresponds to quenching of the higher v' levels, whereas the slowly decaying component corresponds to quenching of the lowest v' levels. This result is in strong contrast to results published for photolysis of HN_3 or HNCO in these same wavelength regions, in which NH was produced in only the $^1\Delta$ state with <u>no</u> vibrational excitation.[3,33,34] The vibrational excitation of the $b^1\Sigma^+$ state of NCl may be rationalized by comparing the NCl bond lengths in ClN_3 and NCl$(b^1\Sigma^+)$. The bond length in ClN_3 corresponds to the internuclear distance for $v' = 9$ in the $b^1\Sigma^+$ state; hence,

if optical excitation occurs by a vertical Franck-Condon transition, it is not surprising that vibrationally excited NCl ($b^1\Sigma^+$) is produced. This situation does not occur in HN_3 or HNCO.

The observation of emission from the $b^1\Sigma^+$ state of NCl suggests that the lowest lying excited singlet state, the $a^1\Delta$ state may also be produced by the photodissociation process. A search for emission from this state near 1.08 μm was fruitless. This is not surprising, however, since the intensity of the $a^1\Delta$ emission is expected to be much lower than that of the $b^1\Sigma^+$ emission, even for comparable densities of the two emitters. A comparison of the spontaneous emission rates for the similar molecules NF and O_2 suggests that the radiative lifetime of the $a^1\Delta$ state may be ~200 times greater than that of the $^1\Sigma^+$ state. When this fact is coupled with the substantially lesser sensitivity of the InAs detector relative to the GaAs PMT, it is not surprising that an NCl ($a^1\Delta$) emission signal was not observed.

Figure 10 shows a diagram which summarizes the results of our experiments on the photodissociation of ClN_3. The measured absorption spectrum is shown along the vertical energy scale, and transitions from the ground state of ClN_3 (X^1A') are indicated by arrows. The oscillatory lines indicate non-radiative processes. Note that the ground states of the NCl and N_2 fragments lie at energies ~11,000 cm^{-1} lower than that of ground state ClN_3, and the allowed dissociation products NCl ($a^1\Delta$) and $N_2(X^1\Sigma_g^+)$ lie about 2000 cm^{-1} lower. Presumably, there is an energy barrier in the reaction coordinate leading to these products which allows ClN_3 to exist as a metastable species. This metastability was quite evident in the results of our experiments. In the experiments noted above in which NO was added to the system, fully one-third of the NO γ emission occurred at wavelengths shorter than the excitation wavelength for photolysis at 249 nm.

3.3 Collisional Relaxaton of NCl($b^1\Sigma^+$)

As noted above, the pulsed generation of NCl($b^1\Sigma^+$) by photolysis of ClN_3 allows real time techniques to be used for the determination of rate

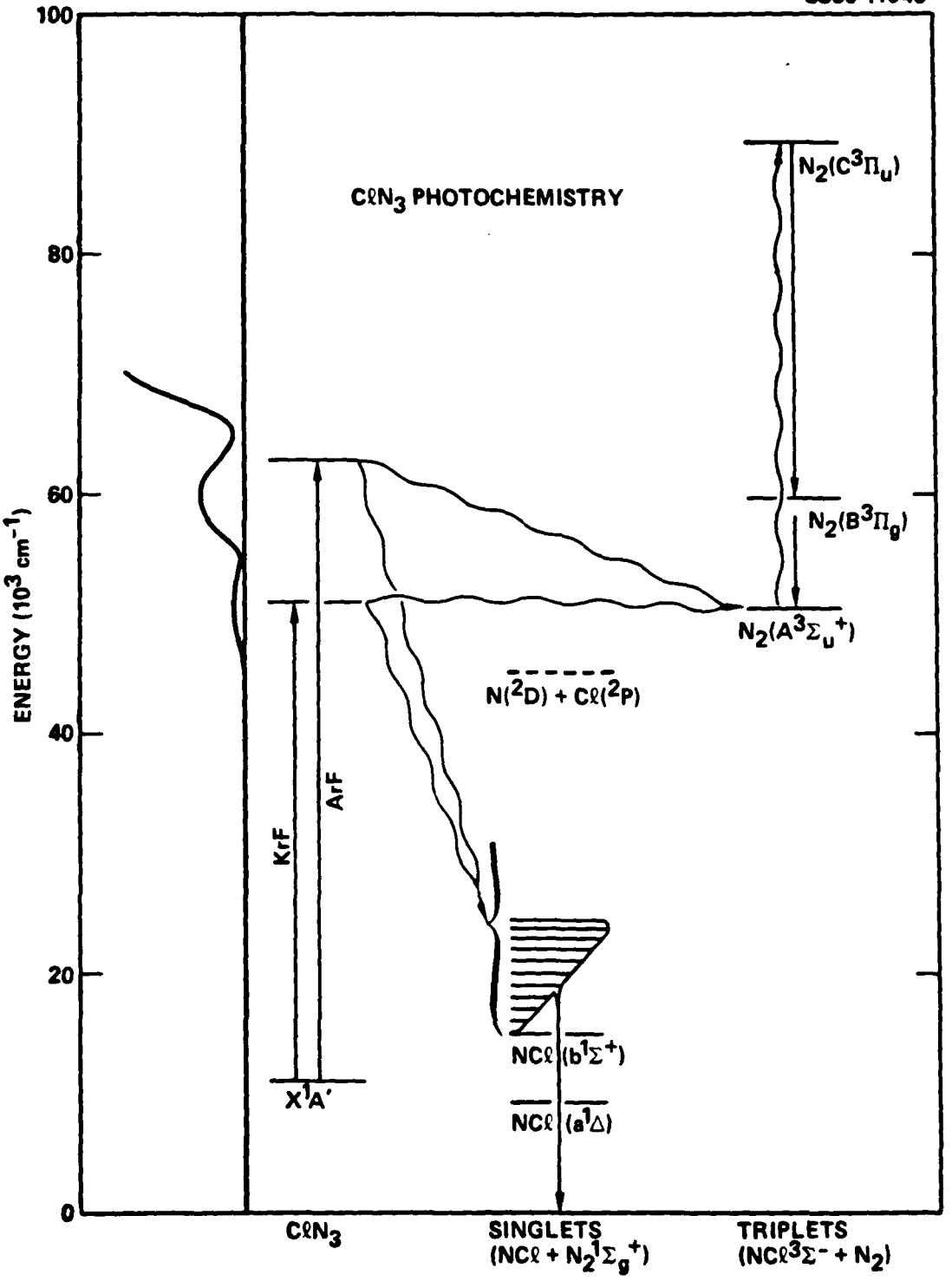

Fig. 10 Energy diagram of the photodissociation of CLN_3 summarizing the observation of the emissions and energy transfer processes.

constants for the collisional quenching of this species. This information is extremely important for assessing the possibility of demonstrating lasers based on $NCl(b^1\Sigma^+)$ emission,[9] and for determining the optimum operating parameters for such devices. Hence, subsequent to the pulsed photolysis experiments discussed above, a series of experiments directed toward measuring quenching rates for a number of relevant species. Measurements were made for several molecular halogens and hydrogen halides, as well as ClN_3, CO_2 and N_2O. Details of this work is given in reference 35 and summarized below.

The total decay rate is given by the following expression:

$$\lambda_{decay} = 1/\tau_{decay} = A + \sum_Q k_Q[Q] + \lambda_{diff} \quad , \tag{21}$$

where A is the spontaneous emission rate, k_Q is the rate constant for collisional quenching by all species (Q) present in the mixture, and λ_{diff} represents the rate of diffusion out of the observation zone. For the conditions of our experiment, the first two terms in Eq. (2) dominate. Decay rates were measured for both the fast ($v' \sim 7$) and slow ($v' = 0$) components of the $NCl(b^1\Sigma^+)$ emission signal. The emission signals were well fitted by single exponentials. According to Eq. (21), the intercept at zero pressure corresponds to the spontaneous emission rate. For the slow component, i.e., the $v' = 0$ level, the radiative rate = 1590 ± 160 sec^{-1} (lifetime = 650 μs). The radiative rate of $v' = 7$ level was found to be $8.0 \pm \frac{9.0}{7.2} \times 10^3$ sec^{-1} or a lifetime of >60 μs. Stern-Volmer plots of Eq. (21) yield linear relationship with the total pressure. If quenching is caused primarily by collisions with undissociated ClN_3 (present at 3.6 mole percent), quenching rate constants for ClN_3 are obtained by dividing the value of the slope by the ClN_3 mole percent. The quenching rate constant obtained in this manner for various v' emitting levels is presented in Table IV.

Table IV. Collisional Quenching f $NCl(b^1\Sigma^+)$[a].

Quencher	$k_{v'}(Q)$, cm^3 $molecule^{-1}$ sec^{-1}[(a)]					
	low v'[b]	v' ~ 2[c]	v' ~ 8[c]	v' ~ 11[c]	v' ~ 15[c]	$\lambda_v > \lambda_e$[d]
Cl_2	1.7×10^{-14}		4.8×10^{-12}			x
ClF	2.7×10^{-12}	1.2×10^{-12}				x
F_2	2.2×10^{-13}					x
ClN_3	1.5×10^{-12}	1.3×10^{-12}	1.3×10^{-11}	4.0×10^{-11}	6.3×10^{-11}	
H_2		2.3×10^{-3}	1.4×10^{-12}			x
HF	1.9×10^{-12}					x
HCl	1.0×10^{-12}					x
CO_2		5.3×10^{-14}	1.2×10^{-13}	4.0×10^{-13}		x
N_2O		1.0×10^{-13}				

a. Here, we have assumed no temperature rise due to photolysis; hence (T = 298K).
b. Measured with a narrow bandpass interference filter centered at 665 nm.
c. Measured with a 0.25 m monochromator set for transitions from these levels.
d. λ_v is the rate of vibrational relaxation in the $b^1\Sigma^+$ state of NCl, and λ_e is the rate of electronic quenching of ClN_3 ($b^1\Sigma^+$) in the lower v' levels.

Quenching experiments for the chaperone gases were performed by addition of known amounts of the quenching gases to the ClN_3/He stream just upstream of the photolysis cell, and measurement of the NCl ($b^1\Sigma^+$) decay time. Quenching rate constants, k_Q, were determined from the following expression:

$$(\lambda_{decay} - A)(P^{-1}) = (k_Q - k_{ClN_3/He})\, X_Q + k_{ClN_3/He} \qquad (22)$$

where X_Q is the mole fraction of the quencher and P is the total pressure in the cell. Overall quenching of the lower v' levels was measured using a narrow band interference filter which selected transitions in the $\Delta v = 0$ sequence. Quenching of the higher v' levels was measured using a 0.25 m monochromator tuned to frequencies corresponding to v' = 2, 8, 11, or 15. In reality, the rate constants measured in these cases correspond to a small range of vibrational levels around these values.

The quenching data obtained in these experiments is presented in Table IV. The primary source of uncertainty in the results shown is the likely presence of impurities in the ClN_3 stream. Some H_2O and HN_3 may be passed by the chemical generator used to produce ClN_3. These molecules may be efficient quenchers of $NCl(b^1\Sigma^+)$, although their concentration is undoubtedly much less than that of ClN_3. This interference would result in errors only if the amounts of these impurities varied during the course of a given measurement.

For a number of the molecules tested, there was evidence of collisionally induced vibrational relaxation within the $b^1\Sigma^+$ state of NCl. This phenomenon was indicated by a slight rise in the intensity of emission from the lower v' levels just after the laser pulse. The magnitude of this effect was dependent on the partial pressure of the chaperone gas. In some cases, there was evidence that the higher v' levels in $ClN_3(b^1\Sigma^+)$ underwent electronic quenching at an enhanced rate. In particular, $NCl(b^1\Sigma^+)$ quenching by ClN_3 showed no evidence of vibrational relaxation. The data shown in Table IV for this system can be approximately fitted to the following expression:

$$k_Q = Z\, e^{-E_a kT}\, e^{\alpha E_v/kT} \quad , \tag{23}$$

where Z is the gas kinetic collision rate, E_a is the activation energy for quenching of $NCl(b^1\Sigma^+)$ v' = 0, and α is a fraction representing the degree to which additional energy in vibration (E_v) enhances the rate. For quenching by ClN_3, this analysis yields $E_a = 3.4 \pm 0.2$ kcal/mole, and $\alpha = 0.10 \pm 0.02$.

Quenching of $NCl(b^1\Sigma^+)$ by the (inter)halogen species Cl_2, ClF, and F_2 may also involve a reactive channel, since the formation of the nitrogen dihalide is exothermic with each of these compounds. Quenching of $NCl(b^1\Sigma^+)$ by the hydrogen compounds given in Table IV or by CO_2 and N_2O would be unreactive. The rate constants associated with H_2, HF, and HCl suggest that perhaps near resonant E-V processes may play a role as follows:

$$H_2 \rightarrow NCl(a^1\Delta, v = 1) + H_2 (v = 1) \qquad (24a)$$

$$NCl(b^1\Sigma) + HF \rightarrow NCl(a^1\Delta, v = 1) + HF (v = 1) \qquad (24b)$$

$$HCl \rightarrow NCl(a^1\Delta, v = 0) + HCL (v = 2) \qquad (24c)$$

3.4 Rate Constants for F and Cl Atom Reaction with HN_3

From our chemiluminescence flow tube experiments, we inferred that the rate constant for the F + HN_3 reaction must be greater than 1×10^{-11} cm^3 s^{-1}, and that for Cl + HN_3 must be $\leq 1 \times 10^{-11}$ cm^3 s^{-1}. This difference could qualitatively be explained within an RRK framework in which the more exothermic channel which, in this case, would arise from the F + HN_3 reaction would be the faster one, assuming comparable activation barrier for the two reactions. Since these rate constants were only indirectly obtained, it was necessary to firmly establish these values before a more definitive interpretaton of the results could be reached.

Both of these reactions have sufficient energy to produce vibrational excited HX species. Sloan and co-workers determined that the vibrational distribution in the F + HN_3 reaction was statistical, with HF (v = 1) the most populated vibrationally excited component. The Cl + HN_3 reaction has sufficient energy to populate v = 2 in HCl. By following the HX(v) emission time profile in the pulsed photolysis apparatus, we could determine these rate

constants. The details of the experiment, including the data analysis and results are presented in Appendix B in manuscript form for submisson to J. Chem. Phys.

The room temperature halogen atom reaction rate constants are 1.6×10^{-10} cm^3 s^{-1} and 1.3×10^{-12} cm^3 s^{-1} for the F + HN_3 and Cl + HN_3 reactions, respectively. Although these results agree with the conclusions of the chemiluminsecence experiments, the difference is much larger than originally thought. Instead of a rate constant ratio ~10, it is ~100, suggesting that the exothermicity of the exit channel alone cannot explain the rate constant ratio. Consequently, if the RRK theory is to be maintained, the entrance channel to the Cl + HN_3 reaction may have a substantial barrier. Hence, isolating the reaction intermediates, XHN_3, would enable us to establish the correctness of this reaction model.

4. Matrix Isolation Studies of Halogen Atom-Azide Molecule Reactions

Arrested relaxation infrared chemiluminsecence experiments performed by J. J. Sloan and co-workers on the F + HN_3 reaction have indicated that the HF molecules generated by this reaction are produced with a nearly statistical vibrational distribution corresponding to $T_{vib} \approx 7000K$.[21] This result suggests that the reaction proceeds via the formation of an intermediate complex, which has a lifetime sufficiently long for at least partial energy randomization. In light of these results, Sloan et al. performed CNDO calculations to study the nature of potentially bound F - HN_3 species. These calculations indicated strong binding for F atom attack on either of the terminal nitrogens, i.e., to form $HNFN_2$ or HN_2NF. The former molecule seems the more likely given the production of HF in the system. A stable $HNFN_2$ molecule would likely fracture at its weakest bond, in this case the HNF - N_2 bond. Sloan and co-workers therefore hypothesized that HF is formed by elimination from the HNF fragment. These ideas, though reasonable, do not agree well with observations of the F + HN_3 system made in our laboratory. We have directly observed the presence of free N_3 radicals in the reaction mixture using

absorption techniques. Moreover, we have measured high yields of excited NF ($a^1\Delta$) produced by this system,[9] a result which does not seem consistent with the generation of HNF fragments as a significant reaction path.

To resolve this issue, we conducted experiments directed toward trapping stable intermediates of halogen atom - HN_3 reactions in low temperature matrices, such that their structure may be analyzed using infrared spectroscopy. The experiments were performed with the collaboration of Dr. K.O. Christe at the Rocketdyne Division of Rockwell International. The apparatus employed consisted of a Perkin Elmer 283 IR spectrometer and an Air Products DE202S closed cycle helium refrigerator.

The halogen source and HN_3 were co-deposited on a CsI window in a large access of the matrix material. Halogen atoms were produced by irradiation of the matrix through various filters with a 1000 W quartz-haolgen lamp.

Experiments centered on the F_2 - HN_3 system since F_2 is the 'cleanest' source of fluorine atoms for such an experiment. A particular problem arose in this case, however, in that F_2 is a very weak absorber, with an absorption maximum which is overlapped by stronger absorptions in HN_3. The photolysis must be performed at wavelengths substantially longer than the peak of the F_2 spectrum (λ_{peak} ~ 280 nm), where the extinction coefficients are very small ($\lambda \approx 3\ell$ $mole^{-1}$ cm^{-1}). To date, we have observed no changes in the IR spectrum of co-deposited F_2 and HN_3 upon photolysis in this manner. Experiments have been performed in both Ne and N_2 matrices. New features had been observed, however, when the matrices were warmed slightly, allowing migration of the F_2 and HN_3. First, HF absorption is observed in the 3500-4000 cm^{-1} region. In addition, new pairs of bands at 3165 cm^{-1} and 388 cm^{-1}, and 3220 cm^{-1} and 420 cm^{-1}, respectively, grew in. These appeared to be related to the N-H stretch (in HN_3) at 3320 cm^{-1} and the N-N-N in-plane bending mode at 527 cm^{-1},[13] and suggest the formation of an $HF\cdots HN_3$ moiety. Further evidence to this effect was found in an increase in the NH deformation frequency from 1270 cm^{-1} (in HN_3) to ~1432 cm^{-1}; the 1432 band is obscurred, however, by numerous N_3 featues in the 1400 cm^{-1} to 1600 cm^{-1} region.

This likely observation of a hydrogen bridged compound suggests the possible observation of an analogous F...HN_3 species, were we able to create more F atoms in the matrix. Such a molecule would be most interesting in view of the chemical similarity of HN_3 to hydrogen halides (in particular, HCl and HBr), and the longstanding controversy concerning the observation of neutral XHY molecules in matrix isolation experiments performed by Pimentel and co-workers.[26] Most recently, Ault has investigated the possible existence of FHF and FHCl molecules in a matrix environment.[32]

PUBLICATIONS

1. A.T. Pritt, Jr. and R.D. Coombe, "Azide Mechanisms for the Production of NCl Metastables," Int. J. Chem. Kinetics 12, 741 (1980).

2. A.T. Pritt, Jr., D. Patel and R.D. Coombe, "Visible and Near-Infrared Electronic Transitions in NCl and NBr," J. Mol. Spectrosc. 87, 401 (1981).

3. R.D. Coombe, D. Patel, A.T. Pritt, Jr. and F.J. Wodarczyk, "Photodissociation of ClN_3 at 193 and 249 nm," J. Chem. Phys. 75, 2177 (1981).

4. A.T. Pritt, Jr., D. Patel and R.D. Coombe, "Decay Kinetics of $NCl((b^1\Sigma^+,v')$," J. Chem. Phys. 75, 5720 (1981).

5. A.T. Pritt, Jr. and D. Patel, "Rate of Reactions for F and Cl Atoms with HN_3," to be submitted to J. Chem. Phys,

6. A.T. Pritt, Jr. and D. Patel, "Rotational Analysis of the 0-0 Band of the b-X Transition in NBr," to be submitted to J. Mol. Spectros.

ORAL PRESENTATIONS

1. R.D. Coombe and A.T. Pritt, Jr., "Excited State Chemistry of the Halogen Azides," AFOSR Molecular Dynamics Conference, U.S. Air Force Academy, Colorado, October, 1979.

2. R.D. Coombe, "Chemical Generaton of Excited Nitrogen Halides," 10th Winter Colloquium in Quantum Electronics, Snowbird, Utah, January, 1980.

3. A.T. Pritt, Jr., D. Patel and R.D. Coombe, "Visible and Near IR Electronic Transitions in NCl and NBr," 35th Symposium on Molecular Spectroscopy, Ohio State University, Columbus, Ohio, June, 1980.

4. A.T. Pritt, Jr., "The Search for Visible Chemical Laser", Rockwell International Science Center, Thousand Oaks, CA, June, 1981.

5. D. Patel, "Chemical Laser Research," Chemical Physics Seminar, University of Oregon, Eugene, Ore., October 1981.

6. R.D. Coombe, "Photodissociaton of ClN_3 and Decay Kinetics of $NCl(b^1\Sigma^+, v')$," AFOSR Molecular Dynamics Conference, AFWL, Kirtland AFB, Albuquerque, NM, November, 1981.

PERSONNEL

For the first two years (1979- 1981), the principal investigator was R.D. Coombe, but when he departed for employment at the University of Denver, A.T. Pritt, Jr. assumed the role of principal investigator. Other persons performing in this contract were:

Senior Personnel

Dr. K. O. Kirste

Dr. F. J. Wodarczyk

Junior Personnel

Mr. R. K. Horne

Mr. J. Patel

Mr. D. Strauss

REFERENCES

1. H. Okabe, J. Chem. Phys. 49, 2726 (1968).

2. J.R. McDonald, J.W. Rabalais and S.P. McGlynn, J. Chem. Phys. 52, 1332 (1970).

3. J.R. McDonald, R.G. Miller and A.P. Baranovski, Chem. Phys. Lett. 51, 57 (1977).

4. R.S. Koran, S. Matsumoto an B. De B. Darwest, Trans. Faraday Soc. 67, 1698 (1971).

5. R.S. Paur and E.J. Blair, Int. J. Chem. Kinetics 8, 139 (1976).

6. T.C. Clark and M.A.A. Clyne, Trans. Faraday Soc. 66, 877 (1969).

7. T.C. Clark and M.A.A. Clyne, Trans. Faraday Soc. 65, 2994 (1969).

8. R.D. Coombe and A.T. Pritt, Jr., Chem. Phys. Letts. 58, 606 (19).

9. R.D. Coombe, D. Patel, A.T. Pritt, Jr. and F.J. Wodarcyzk, AFWL Final Report for Contract F29601-79-C-0016, Rockwell International Science Center, Thousand Oaks, CA 91360.

10. D.E. Milligan and M.E.Jacox, J. Chem. Phys. 40, 2461 (1964).

11. E. Gystein an J.F. Haller, Appl. Spectrosc. 20, 417 (1966).

12. R.D. Coombe and A.T. Pritt, Jr., unpublished results, 1978.

13. A. Fontijn, C.B. Meyer and H.I. Schiff, J. Chem. Phys. 40, 64 (1964).

14. P.S. Ganguli and M. Kaufman, Chem. Phys. Lett. 25, 221 (1974).

15. L.W. Strattan and M. Kaufman, J. Chem. Phys. 66, 4963 (1977).

16. D.A. Dows and G. Pimental, J. Chem. Phys. 23, 1258 (1955).

17. J.R. MacDonald, J.W. Rabalais and S.P. McGlynn, J. Chem. Phys. 52, 1332 (1970).

18. D.A. Spencer, J. Chem. Soc. 217 (1925).

19. J.M. Herbelin and N. Cohen, Chem. Phys. Lett. 20, 605 (1973).

20. R. Colin and W.E. Jones, Canad. J. Phys. 45, 301 (1967).

21. J.J. Sloan, D.G. Watson and J.S. Wright, Chem. Phys. 43, 1 (1979).

22. A.T. Pritt, Jr. and R.D. Coombe, Int. J. Chem. Kinetics 12, 741 (1980).

23. R.A. Ashby and R.L. Werner, J. Mol. Spectrosc. 18, 184 (1965).

24. A.G. Briggs and R.G.W. Norrish, Proc. Roy. Soc. A278, 27 (1964).

25. A. Elliot, Proc. Roy. Soc. A169, 469 (1939).

26. E.R.V. Milton, H.B. Dunford and A.E. Douglas, J. Chem. Phys. 35, 1202 (1961).

27. A.T. Pritt, Jr., D. Patel and R.D. Coombe, J. Mol. Spectrosc. 87, 401 (1981).

28. S. Itagi, N.R. Shamkuwar and V.V. Itagi, Indian J. Phys. 45, 385 (1971).

29. K. Dehnicke and P. Ruschke, Z. Naturforsch. 33B, 750 (1978).

30. C. Schack and R. Wilson, private communication, 1976.

31. R.D. Coombe, D. Patel, A.T. Pritt, Jr. and F.J. Wodarczyk, J. Chem. Phys. 75, 2177 (1981).

32. W.G. Clark and D. Setsen, J. Chem. Phys. 84, 2225 (1980).

33. A.P. Baranovski, R.G. Miller and J.R. McDonald, Chem. Phys. 30, 119 (1978).

34. W.S. Droydoski, A.P. Baranovski and J.R. McDonald, Chem. Phys. Lett. 64, 421 (1979).

35. A.T. Pritt, Jr., D. Patel and R.D. Coombe, J. Chem. Phys. 75, 5720 (1981).

36. See, for example, V. Bondybey, G.C. Pimentel and P.N. Noble, J. Chem. Phys. 55, 540 (1971).

37. B.S. Ault, J. Chem. Phys. 68, 4012 (1978).

APPENDIX A

ROTATIONAL ANALYSIS OF THE 0-0 BAND IN THE NBr $b^1\Sigma^+$-$X^3\Sigma^-$ TRANSITION

A.T. Pritt, Jr. and D. Patel
Rockwell International Science Center
1049 Camino Dos Rios
Thousand Oaks, CA 91360 USA

ABSTRACT

Rotationally resolved emission spectra of the 0-0 band of the $b^1\Sigma^+$-$X^3\Sigma^-$ transition in NBr were obtained from the F/Br + HN_3 chemiluminsecence flame. The spectra revealed two strong branches, the ^SR and ^QP, and two much weaker branches, the ^OP and ^QR, with the ^QQ branch unobserved. The resolution of the apparatus was not sufficient to resolve the two naturally occurring isotopes of Br. Analysis of these rotational lines yield the following set of molecular constants:

ν_{00} = 14824.3 ± 2 cm^{-1}
B_0' = 0.4712 ± 0.0010 cm^{-1}
B_0'' = 0.4455 ± 0.0013 cm^{-1}
λ = 12.71 ± 0.14 cm^{-1}
γ = 0.0599 ± 0.0004 cm^{-1}

Introduction

In an earlier publication we reported on the visible $b^1\Sigma-X^3\Sigma^-$ and near infrared $a^1\Delta-X^3\Sigma^-$ bands of NCl and NBr.[1] The $b^1\Sigma^+-X^3\Sigma^-$ system of NBr exhibited a double headed feature in which the blue-shifted band head is much more intense. Milton, Dunford and Douglas[2] obtain rotationally resolved spectra on the b-X transition in NBr for the higher v' bands (v' = 3-9). These authors reported that the stronger of these band-heads consisted of a ^QP and ^SR branches which corresponded to transitions terminating on the F_1(=N+1) component of the $X^3\Sigma^-$ state. They were unable to observe any other branches, and therefore were unable to report accurate values for the spin-spin, λ, and spin-rotation, γ, constants.

In this paper we have obtained rotationally resolved spectra for the 0-0 band of the b-X transition in NBr. In particular we have obtained and analyzed the rotational lines associated with the weaker band head system, verifying that the weaker band does indeed consist of the "missing" transition reported by Milton et al. Moreover, from the analysis of the four branches we report accurate values for λ and γ. In our analysis of the low resoltuion vibrational spectra of the b-X emission, we suggested that the weaker red-shifted bands were part of the b-X system, namely, consisting of the ^OP and ^OR branches, corresponding to transitions terminating on the F_3(=N-1) component of the $X^3\Sigma^-$ state. Furthermore from the relative positions of the two band heads and their intensity ratio, we inferred that one set of values for λ and γ provided a reasonable description of the 0-0 band emission.

Experimental Details

The apparatus for generating the NBr flame has been described elsewhere (1,3,4). Briefly, streams of atomic fluorine are produced by passage of molecular fluorine diluted in argon through a microwave cavity and into the outer annulus of a triply concentric flow tube assembly. Nitrogen is bubbled through liquid bromine at atmospheric pressure and passed through the inner annulus of the flow tube. The molecular bromine reacts with the atomic fluor-

ine producing atomic bromine and BrF; the reverse reaction Br + F_2 is very slow.[5] Hydrogen azide is passed through the innermost tube and injected 10 cm downstream of the point where molecular bromine is admitted. The HN_3 is injected through a single small hole forming a vertical flame.

The flame was focused onto the entrance slit of a 1 meter monochromator (Interactive Technology Model CT103) equipped with a 6-inch square 1200 line/mm blazed at 500 nm, and the dispersed emission was detected by a cooled GaAs photomultiplier tube (RCA C31034). The photoelectric pulses were amplified, discriminated and sent both to an SSR photon counting computer and to a Nicolet Signal Averager (Model 1170) operating in its multichannel analyzer mode. Some spectra were also taken on a stripchart recorder. The wavelength position of the monochromator was calibrated against atomic neon lines, but not when the NBr spectra was obtained. Reproducibility in the wavelength scan was ~ ±0.1 nm, representing ~ ±2 cm^{-1} in the ν_{00} value. The slits were typically set at 12 μm which for the monochromator alignment yielded a resoltion of ~0.5 cm^{-1}. The precision on determining an overlapped line ~0.1 cm^{-1}.

Data Analysis and Results

The rotationally resolved spectra of the 0-0 band is shown in Fig. A1. The lines associated with a less intense band is on the order of seven times weaker than those of the stronger branches.

The ^{Q}R and ^{O}P branches do not overlap and, therefore, are easily resolved as shown in Fig. A2. Unfortunately, the intensity of these bands decreases dramatically with decreasing J values. Since the important $^{O}P(1)$ and $^{Q}R(1)$ lines are unobserved, a straightforward assignment is difficult. An assignment, however, can be made by plotting combination differences,

$$\Delta_2 F(J) = 4B_0' \left(J + \frac{1}{2}\right) \qquad (1)$$

against selected J values until two conditions are met: the zero combination difference corresponds $J = -1/2$, and the slope yields a B_0' value in agreement with the value reported by Milton et al. For the assignment of the individual lines given in Table A-I, the value of B_0' was found to be 0.4712 ± 0.0010 cm^{-1}, and $J = -0.67 \pm 0.13$ for $\Delta_2F_3 = 0$. From the values of Be and α_e reported by Milton et al., $B_0' = 0.4713$ cm^{-1}. Other assignments for the ^OP and ^QR branches gave $\Delta_2F_3 = 0$, J values near -1/2 but the B_0' value was found to exceed values of 0.48 cm^{-1} or less than 0.465 cm^{-1}. In a like manner, the ^SR and ^QR branches were also determined. The assignments and individual vacuum wavenumber lines are reported in Table A-I.

The upper state B value was determined in the usual way by a one parameter linear least squares fit of equation (1). The analysis was extended to second order to determine D, but the magnitude of the 1σ error exceed the value of D, indicating that for the range of ΔF values given the deviation from a linear one parameter fit did not exceed the precision of the data.

The lower state needs an additional two parameters, λ and γ, to approximately describe its rotational levels. J. K. G. Watson[6] derived the following formulae for the three sublevels of the $X^3\Sigma$ state

$$F_1'(J) = B' J(J+1) + (2\lambda-\gamma) + (B' - \lambda-1/2\gamma) - \alpha(J) \quad (2)$$

$$F_2'(J) = B' J(J+1) + (2\lambda-\gamma) \quad (3)$$

$$F_3(J) = B' J(J+1) + (2\lambda-\gamma) + (B' - \lambda-1/2\gamma) + \alpha(J) \quad (4)$$

where,

$$\alpha(J) = [(B - \lambda-1/2\gamma)^2 + 4J(J+1)(B-1/2\gamma)^2]^{1/2} \quad (5)$$

The term $(2\lambda-\gamma)$ is typically contained in the value of ν_{00} as we have done in this analysis.

Using the following relationship

$$S_{R(J-1)} - {}^{Q}P_{(J+1)} + {}^{Q}R_{(J-1)} - {}^{O}P_{(J+1)} = 8B'_{0}(J+1/2) \qquad (6)$$

The value of B''_0 was determined again as was done for the upper state constant by a one parameter least squares fit of the measured lines. Unfortunately, only six data points were used to determine B'_0. Extending the analysis to include higher order terms again resulted in a magnitude of the error greater than that of its value. Hence, only one constant was determined and is reported in Table A-III.

It can be shown that

$$\alpha(J) = \frac{1}{2}\left[{}^{S}R(J) - {}^{Q}R(J)\right] = \frac{1}{2}\left[{}^{Q}P(J) - {}^{O}P(J)\right] \qquad (7)$$

and therefore plots of $\alpha^2(J)$ vs $J(J+1)$ yield a slope = $(B-1/2)^2$ and an intercept $\frac{1}{4}(B - \lambda - 1/2\gamma)^2$. It can be readily seen that two values of γ are obtained depending on which root is taken. Furthermore, for a given value of γ two possible values of λ are obtained. The possible combination of values is given in Table A-II.

Since the ${}^{Q}Q$ branch is not observed in these spectra, we are unable to assign the sign of λ. In the b-X transition of NF, the ${}^{Q}Q$ band head is observed and leads to a positive value for λ. In similar isoelectronic molecules, λ is positive and therefore, we have chosen a positive value for λ. In addition, the best value of γ for NF[7] and NCl[8] are reported to be $-0.00048\ cm^{-1}$ and $-0.0072\ cm^{-1}$, respectively. In following the trend, we have selected the values for λ and γ reported in Table A-III.

We have taken these experimentally determined constants (ν_{00}, B'_0, B'_0, λ and γ) and have calculated all of the line positions and compared them to the observed values. The reduced chi square value ($\bar{\chi}^2$)

$$\chi^{-2} = \frac{\sum_i (y_{obs}-y_{calc})_i^2}{N-5}$$

was determined to be 0.08 $(cm^{-1})^2$. The above analysis was performed for a variety of different J assignments for the various branches, but only one unique assignment produced a reduced chi square <0.1 cm^{-1}; all others exceeded 0.9 cm^{-1}.

Discussion

From the analysis of the weaker red-shifted band bead system, it is clear that these branches are the ^{O}P and ^{Q}R branches associated with the 0-0 band. These transitions terminate in the $F_3(N=N-1)$ levels. Search for those lines terminating on $F_1(J=N)$, i.e., the ^{Q}Q branch associated with the $\Omega=1^+$ level proved fruitless. Hence, the transition moment (μ_1) perpendicular to the internuclear axis is much smaller than that (μ_0) parallel to it.

The molecular constants for the v=0 levels of the $b^1\Delta$ amd $X^3\Delta^-$ state of NF, NCl and NBr are presented in Table A.III. The spin-spin and spin-rotation constants, as expected, increased with the mass of the halogen atom. This series can be contrasted by the three Group V-Fluorides in which λ = 1.22, 29.6, 69.66 cm^{-1}, respectively for NF,PF,and AsF. The value of γ for the Group V-Fluoride increases much faster than that for the corresponding nitrenes. Another difference between these two series is the ratio of the magnitude of the two transition moments μ_1/μ_0. For NCl and NBr, this ratio is vanishing small, whereas for PF and AsF, this ratio is near unity given the intensity of the ^{Q}Q branch relative to others four branches. The intensity of the ^{O}P and ^{Q}R branches ($\Omega=1^+$) relative to that of the ^{Q}R and ^{Q}P branches ($\Omega=0^+$) agree well with the intensity relationships given by Watson. The rotational constant for both the $b^1\Sigma$ and $X^3\Delta^-$ states of NBr agree well with the extrapolated values of Milton et al. of 0.4713 and 0.444 cm^{-1}, respectively.

REFERENCES

1. A. T. Pritt, Jr., D. Patel, R. D. Coombe, J. Mol. Spectrosc. 87, 401 (1981).

2. R. V. Milton, N. B. Danford, and A. E. Douglas, J. Chem. Phys. 35, 1202 (1961).

3. R. D. Coombe and A. T. Pritt, Jr., Chem. Phys. Lett. 58, 606 (1978).

4. A. T. Pritt, Jr., D. Patel and R. D. Combe, Int. J. Chem. Kinetics 12, 741 (1980).

5. L. W. Strattan and M. Kaufman, J. Chem. Phys. 66, 4963 (1977).

6. J. K. G. Watson, Canad. J. Phys. 46, 1637-1643 (1968).

7. A. E. Douglas and W. E. Jones, Can. J. Phys. 44, 2251 (1966).

8. R. Colin and W. E. Jones, Can. J. Phys. 45, 301 (1967).

Table A-I. Vacuum Wave Numbers of the Lines of the NBr 0-0 Band.

J	$O_P(J)$	$Q_R(J)$	$Q_P(J)$	$S_R(J)$
1				
2	14810.94			14840.68
3	9.45			42.12
4	8.48	14817.33		42.83
5	7.44	18.05		43.43
6	6.32	18.82		45.30
7	5.24	19.64		47.04
8	4.18	20.53		48.88
9	3.12	21.37		50.90
10	2.17	22.29	14832.99	52.86*
11	1.06	23.18	33.33	55.39*
12	0.01	24.06	33.71	57.26*
13	14799.10	24.92	33.91	57.48*
14	98.21	25.89	34.41	61.85*
15	97.32	26.85	35.00	64.30
16	96.41	27.92	14835.94	66.79*
17	95.60	28.89	36.60	69.30*
18	94.82	29.95	37.31	72.00
19	94.06	31.06	38.22	74.66
20	93.41		39.17	77.25*
21	92.75		40.12	80.19*
22	92.12		40.95	83.09
23	91.63		42.11	86.15
24	90.67		43.38	89.15
25	89.82		44.45	
26			45.57	
27			47.02	
28			48.33	

Table A-I (Continued)

J	$O_{P(J)}$	$Q_{R(J)}$	$Q_{P(J)}$	$S_{R(J)}$
29			14848.75	
30			51.24	
31			52.86*	
32			54.53*	
33			55.97	
34			57.79*	
35			59.56*	
36			61.28*	
37			63.02	
38			64.97*	
39			66.76*	
40			68.72*	
41			71.11	
42			73.11	
43			75.46*	
44			77.29*	
45			80.19*	
46			82.29*	
47			84.55	

* Overlapping lines.

Table A-II. Possible Values For λ and γ.

	A	B
λ (cm^{-1})	± 12.71	± 11.22
γ (cm^{-1})	-0.0599	+ 1.840

Table A-III. Molecular Constants for the v=0 Levels of the $b^1\Delta^+$ and $X^3\Delta^-$ States of the Halogen Nitrenes.

		NF[a]	NCl[25 b]	NBr[c]
$b^1\Sigma^+$:	ν_{oo}	18905.20	15038.94	14824.3
	B_o	1.23052	0.68284	0.4712
	D_o	5.28×10^{-6}	1.65×10^{-6}	-------
$X^3\Sigma^-$:	B_o	1.19834	0.64685	0.4455
	D_o	5.39×10^{-6}	1.78×10^{-6}	-------
	λ	1.21	1.776	12.71
	γ	0.0048	-0.00715	-0.0599

a. Reference 7.
b. Reference 8.
c. This work

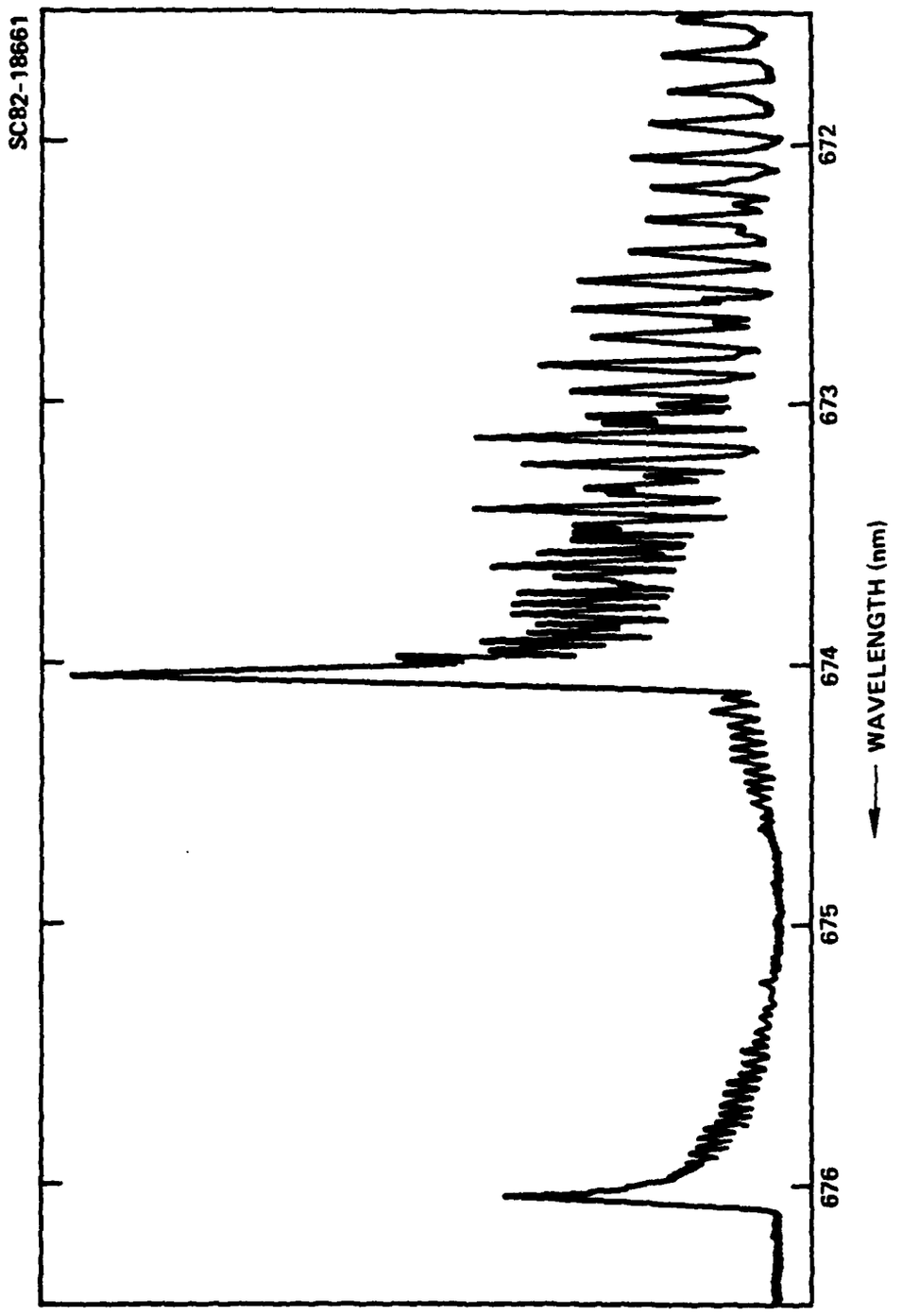

Fig. A1 Spectrum of the 0-0 band of the NBr b-X transition.

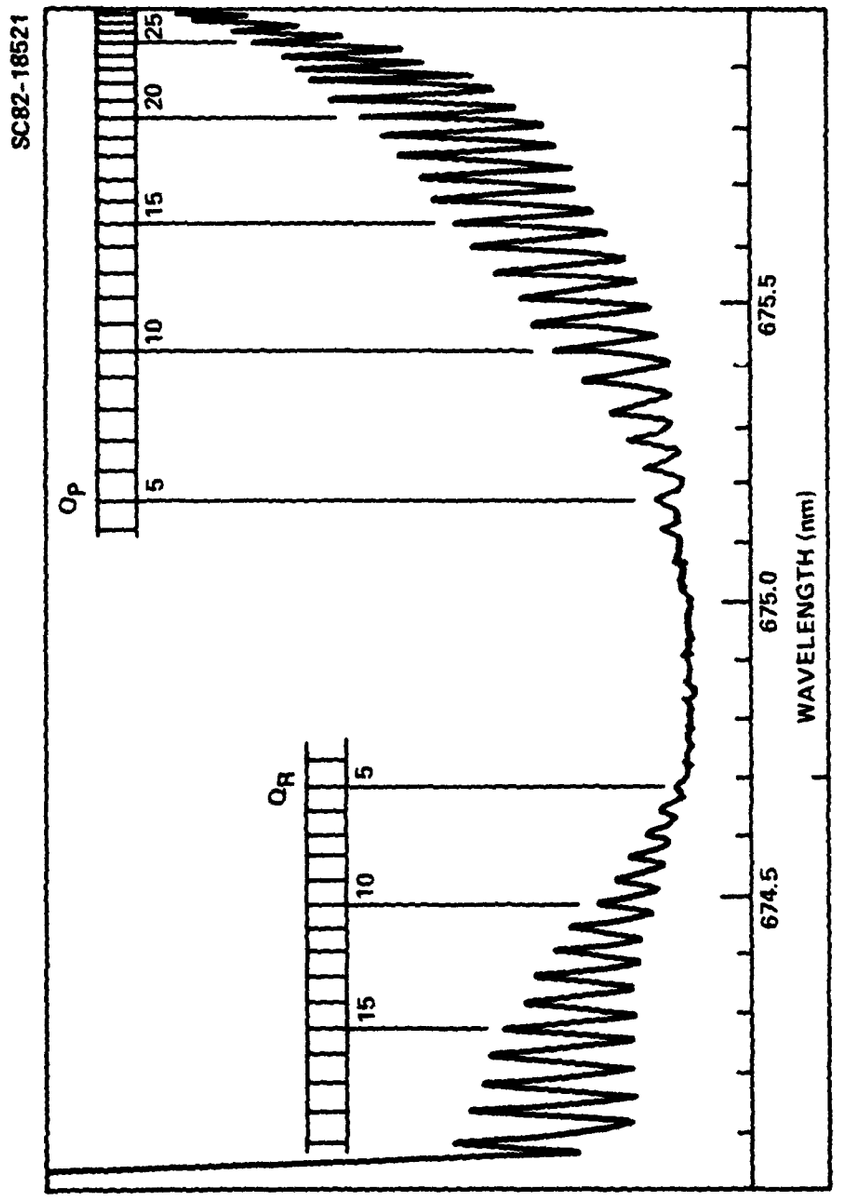

Fig. A2 Spectrum of the O_P and O_R branches of the 0-0 band of the NBr b-X transition.

APPENDIX B

REACTION RATE OF F AND Cl ATOMS WITH HN_3

A.T. Pritt, Jr. and D. Patel

Rockwell International Science Center
1049 Camino Dos Rios
Thousand Oaks, CA 91360 USA

ABSTRACT

The total reaction rate of F and Cl atoms with HN_3 was determined by real-time analysis of the product vibrational fluorescence following pulsed laser photolysis of F_2 and Cl_2. Plots of reaction rate vs. HN_3 concentration yield room temperature rate constants of $1.6 \pm 0.3 \times 10^{-10}$ cm^3 s^{-1} and $1.3 \pm 0.3 \times 10^{-12}$ cm^3 s^{-1} for the F and Cl atom reactions, respectively. The results are interpreted in an RRK framework.

Introduction

Halogen atom reactions with hydrogen containing molecules have been studied for a number of different systems, spurred by the development of infrared chemical lasers. These reactions are typified either by hydrogen abstraction resulting in an inverted vibrational product distribution of the hydrogen halide, or by an insertion-elimination mechanism resulting in a statistical vibrational distribution. Examples of the abstraction reaction are X + HY, where X and Y are halogen atoms,[1-3] whereas examples of the latter include F-atom reactions with alkenes,[4] HN_3[5] and HNCO.[6] Recently, Sloan et al.[5] determined that the HF vibrational distribution in the F + HN_3 reaction was statistical having a vibrational temperature of ~7000K. CNDO calculations show that the strongest attractive potential for the F-atom approach occurs at the terminal nitrogen and the hydrogenated nitrogen. Given the statistical nature of the distribution and the exothermicity of the reaction determined by the highest energy levels observed in the product molecule, HF, these authors concluded that the primary route to dissociation was the initial formation of HNF + N_2 with a subsequent elimination of HF. This conclusion is entirely within the scope of the usual unmolecular decay mechanism in that the energy of the reaction is entirely randomized over the degrees of freedom of the intermediate complex with breakage at the weakest bond.

In chemiluminescence flow tube experiments performed in our laboratories, we have suggested that the mechanism by which NF ($a^1\Delta$) is produced in the F + HN_3 reaction system is via an azide radical intermediate.[7] Moreover, in subsequent studies, we have determined that under conditions of excess F-atom relative to NF ($a^1\Delta$) in the limit of very small HN_3 concentrations, the yield of NF($a^1\Delta$) relative to the HN_3 reagent is of the order of unity.[8] In addition, we have observed the presence of N_3 in the flow, and from its estimated absorption coefficient,[9] have determined that the N_3 radical must be a significant product channel to the F + HN_3 reaction.

In yet other chemiluminescense flow tube experiments in which Cl atoms are added to the F + HN_3 reaction system, NCl($a^1\Delta$) and NCl($b^1\Sigma$) were

generated.[10] From an indirect analysis of the temporal flame profiles, a lower limit for the rate constant of F + HN_3 is 1×10^{-11} cm^3 s^{-1} and an upper limit to the Cl and HN_3 reaction is 1×10^{-12} cm^3 s^{-1}, implying that the ratio of the F + HN_3 rate constant to that for the Cl + HN_3 reaction exceeds 10. The lower limit for the F + HN_3 reaction comes from the time resolution of the experiment, and from the rate of mixing associated with these experiments. The upper limit on the Cl + HN_3 reaction has a large degree of uncertainty, but thought to be within a factor of three of the true value. We rationalized these results in terms of an RRK model by suggesting that the exothermicity difference in these two halogen atom reactions, assuming negligible activation energies, could account for the observed rate constant ratio. Hence, this results supports the view held by Sloan et al.[5] in which the major product channel does not generate N_3, and therefore at odds with the observed magnitude of the N_3 absorption signal.[8]

In this paper, we have obtained the total rate constant for the reaction of F + HN_3 and Cl+ HN_3 by real-time analysis of the product vibrational fluorescence following pulsed laser photolysis of F_2 and Cl_2, respectively in the presence of excess HN_3 and diluent gas. From the data obtained here and the data of Sloan et al., an attempt at reconciling the apparent contradiction stated above is given. The quenching rate of HF (v=1) by HN_3 is also reported.

Experimental Details

The method of using pulsed laser photolysis of F_2 or CL_2 to generate small concentrations of halogen atoms has been developed by Smith and coworkers.[11] This method must be done in an excess of diluent gases to quickly thermalize the hot atoms produced in the photodissociation step. In our experiments, F or Cl atoms were generated by mildly focusing the output of an XeCl excimer laser (Lambda Physik EMG 101) into a fluorescent cell through which a mixture of F_2 or Cl_2 and HN_3/N_2 gases flowed. Given the concentration of F_2 and Cl_2, the medium was optically thin, absorbing less than 3% of the

laser beam. The beam dimensions in the center of the fluorescent cell was 1.5 × 2.5 cm^2 representing a fluence of ~16 mJ/cm^2. Therefore, the initial F-atom to initial F_2 concentration ratio is less than 0.1%. For photodissociation, Cl_2, this ratio is of the order of 1%.

The T-shaped fluorescent cell was made from a solid block of stainless steel. The laser beam entered and excited the cell via 2" dia. CaF_2 windows sealed to the cell by vitron o-rings. Infrared fluorescence was viewed at right angles to the photolysis path. The fluorescence, after spectral isolation by a narrowband filter, was detected by an InSb element (SBRC, 3 mm dia., cooled to 77K, D* (λ = 5.5 μm)). A silicon flat was positioned between the cell and the detector to further discriminate window fluorescence. For HF fluorescence, the bandpass filter having half transmission points at 2.09 μm and 2.49 μm transmitted ony the R branch of the v = 1 → v = 0 transition. Hence, only the v = 1 level of HF was monitored. The bandpass filter used for HCl transmitted fluorescence between half transmission points of 3.30 μm and 4.67 μm. In the HCl case, therefore, all HCl vibrational levels possible by the reaction were observed. The reaction is only ~2 kcals exothermic. Consequently, the highest vibrational level that could be observed was v = 2. The detector was mated to its own specially designed preamp. After an addition amplification (Hewlett Packard Model 465A), the transient fluorescence signal was captured and digitized by a Biomation 8100 transient recorder. The output of the recorder was sent after each laser pulse to a Northern Pacific signal averger for summing. Once the desired signal-to-noise ratios were obtained, the experiment was stopped and the contents of the signal averager was sent to a PDP 11V03 microprocessor for data storage and eventual analysis.

Gaseous HN_3 was prepared in a manner described in an earlier publication.[7] Briefly, a 75% aqueous H_2SO_4 solution was dropwise added to a bed of solid NaN_3 in a pyrex reaction vessel, while nitrogen gas flowed through the reactor at atmospheric pressure. The HN_3/N_2 mixture then flowed through a Drierite ($CaCl_2$) column and into the fume hood. Infrared spectral analysis of

the gases leaving the drying trap showed only those bands associated with HN_2[12] and no traces of the H_2O bands, verifying that the concentration of H_2O was less than 10% of that of HN_3. A small portion of the flow was directed through a mass flowmeter and into an absorption cell, where the optical density of HN_3 was monitored with the aid of a D_2 lamp, monochrometer and PMT assembly. The total pressure in the cell was monitored by a Validyne inductance manometer. From the reported extinction coefficient of HN_3 (λ = 205 nm)[13] and the total pressure in the cell, the fraction of HN_3 in the gas mixture was calculated. The HN_3 fraction ranged from 0.4-1.5 $\times$ 10^{-3} for the F + HN_3 experiments, and from 1.0-1.5 $\times$ 10^{-2} for the Cl + HN_3 experiments.

The flow rate of the gases were monitored by mass flowmeters (Tylan), which were calibrated for N_2 flow. The flow rate of F_2 and Cl_2 was determined by multiplying the flow rate readings by a correction factor supplied by the manufacturer. The partial pressure of each constituent was, therefore, determined in the usual way by multiplying the flow rate of that species relative to the total flow rate times the total pressure in the cell. The total flow rate was adjusted to replenish the entire fluorescent cell volume three times every second. In practice, we found that the laser could be operated as high as 10 Hz with no change in the fluorescence time profiles.

Molecular fluorine (Matheson, 98.0%) and molecular chlorine (Matheson, 99.5%) were used directly from the storage tanks without further purification. The N_2 diluent gas (Airco, 99.995%) was also used without any purification.

Data Analysis and Results

The time resolved fluorescence signals could be described by rising and falling exponential of the form,

$$S(t) = |S_0| \left(e^{-\lambda_1 t} - e^{-\lambda_2 t}\right) \qquad (1)$$

where the rate of rise is λ_2 and the rate of fall by λ_1. The rate of the rise of the fluorescence can be either the reaction rate X + HN_3 or the vibrational quenching rate, depending on which is faster. To determine which component in Eq. (1) is the reaction rate, small amounts of CO_2 were added to the flow, since CO_2 rapidly quenches vibrationally excited HF and HCl, but does not interfere with the halogen atom reaction with HN_3. In the F + HN_3 reaction, addition of CO_2 resulted in an acceleration of the HF fluorescence decay, leaving the fluorescence rise time constant until the addition of CO_2 was so great that the fluorescence rise became the quenching rate. Hence, without the presence of CO_2, the rise of the HF fluorescence corresponds to the reaction rate F + HN_3, i.e., to the disappearance rate of F-atoms, since for all these experiments, the concentration of HN_3 was kept at levels in excess of the F-atom concentration. On the other hand, addition of CO_2 did not alter the HCl fluorescence decay rate for the Cl + HN_3 experiments. Consequently, the fluorescence decay rate of HCl corresponds to the Cl + HN_3 reaction rate. Unfortunately, under the conditions of this experiment, the rise time was unresolved, and the quenching rate of HCl was not determined.

The rate of appearance of the $HF^\dagger$ fluorescence is equal to the rate of disappearance of F-atoms since $[HN_3] \gg [F]$. For the pressures used in this experiment and the times associated with HF formation and destruction, diffusion is negligible. Furthermore, F-atom three-body recombinations at these pressures is also much too slow to account for any significant loss of F-atoms. Hence, the rate of $HF^\dagger$ fluorescence rise is solely a function of the F + HN_3 reaction. Plotting the HF fluorescence rate of appearance vs the partial pressure of HN_3 should result in a linear relationship with an Y-intercept at zero. Such a plot is given in Fig. 1. The least squares analysis of this plot gives an intercept of $5.7 \pm 2.5 \times 10^3$ s^{-1} where the uncertainty is an estimated variance based on the goodness of fit. The non-zero intercept indicates that a small F-atom reaction occurs with species contained in the F_2 flow. The rate constant for the F + HN_3 reaction is calculated from the slope of the least squares fit of the data and is reported in the figure.

The rate of $HCl^{\dagger}$ fluorescence decay, as stated above, corresponds to the $Cl + HN_3$, and a plot of this rate vs. the HN_3 partial pressure is shown in Fig. 2. In this case, the zero pressure intercept is zero to within the uncertainty associated with data. The rate constant for $Cl + HN_3$ reaction is determined from the slopes of the linear least squares analysis of the data and is also reported in the figure. Finally, the HF disappearance rate vs HN_3 partial pressure which is plotted in Fig. B3 yields a linear relationship whose slope yields a vibrational quenching rate constant of 6.4×10^{-11} cm^3 $molecule^{-1}$ s^{-1}.

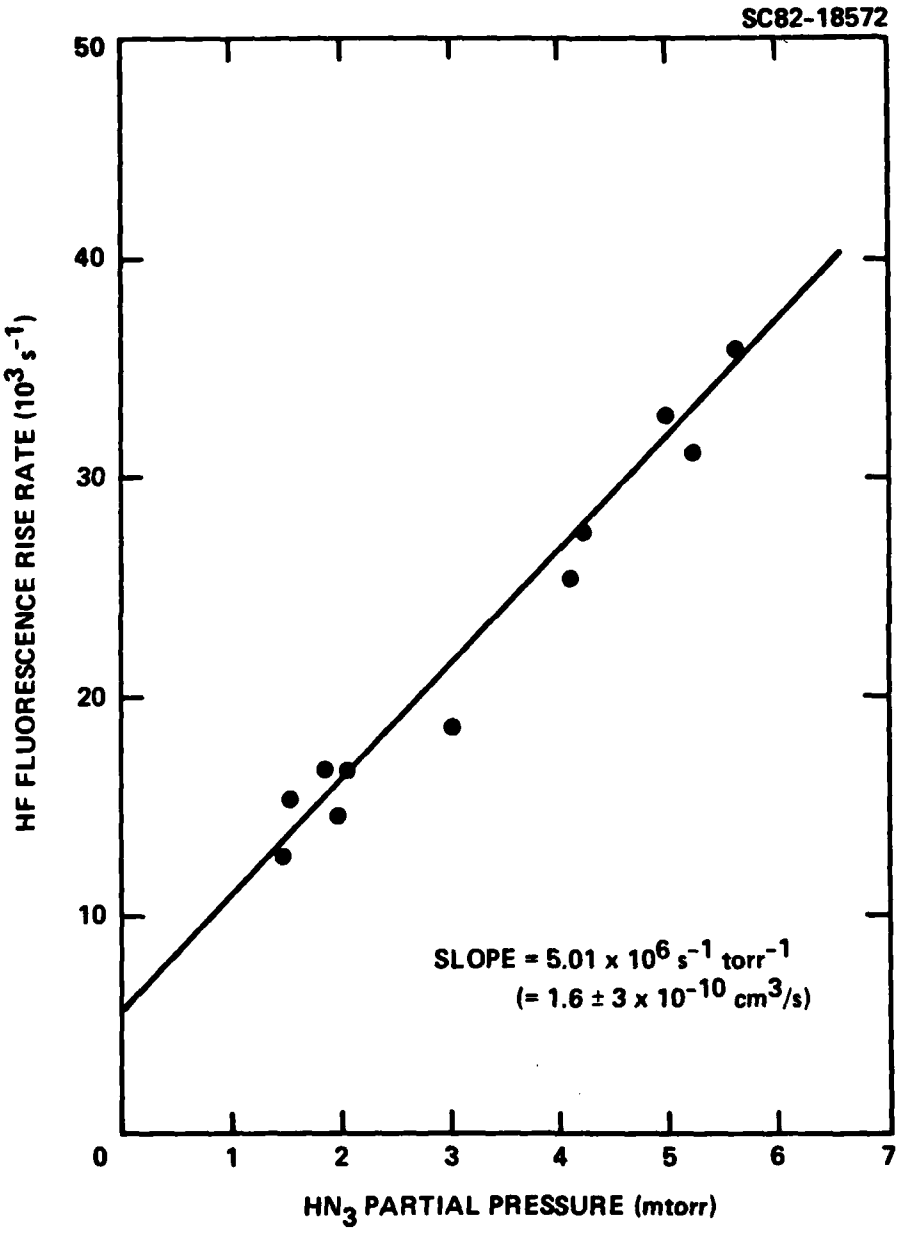

Fig. B1 Plot of the HF fluorescence rise vs HN_3 partial pressure.

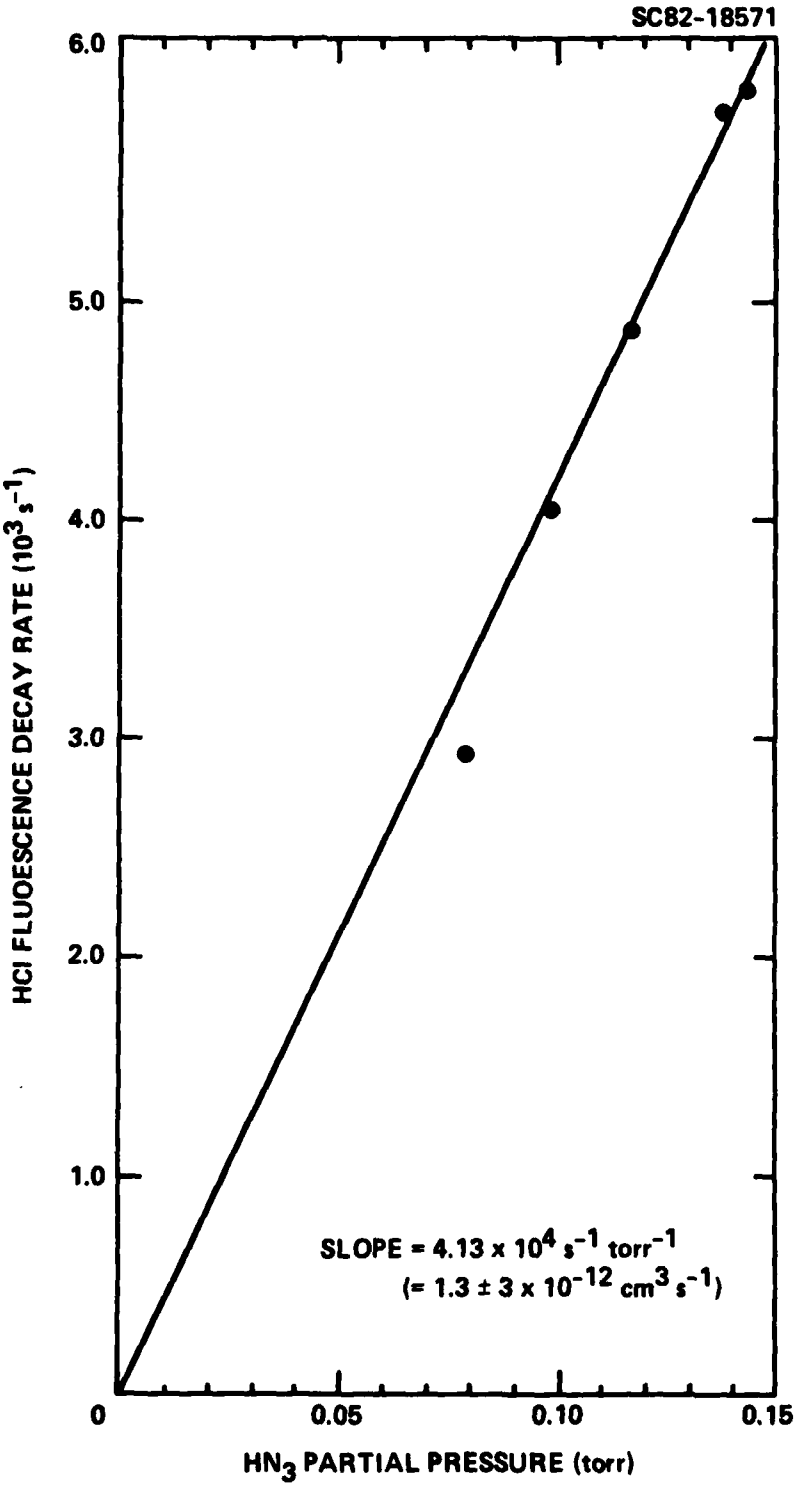

Fig. B2 Plot of the HCl fluorescenje decay vs HN_3 partial pressure.

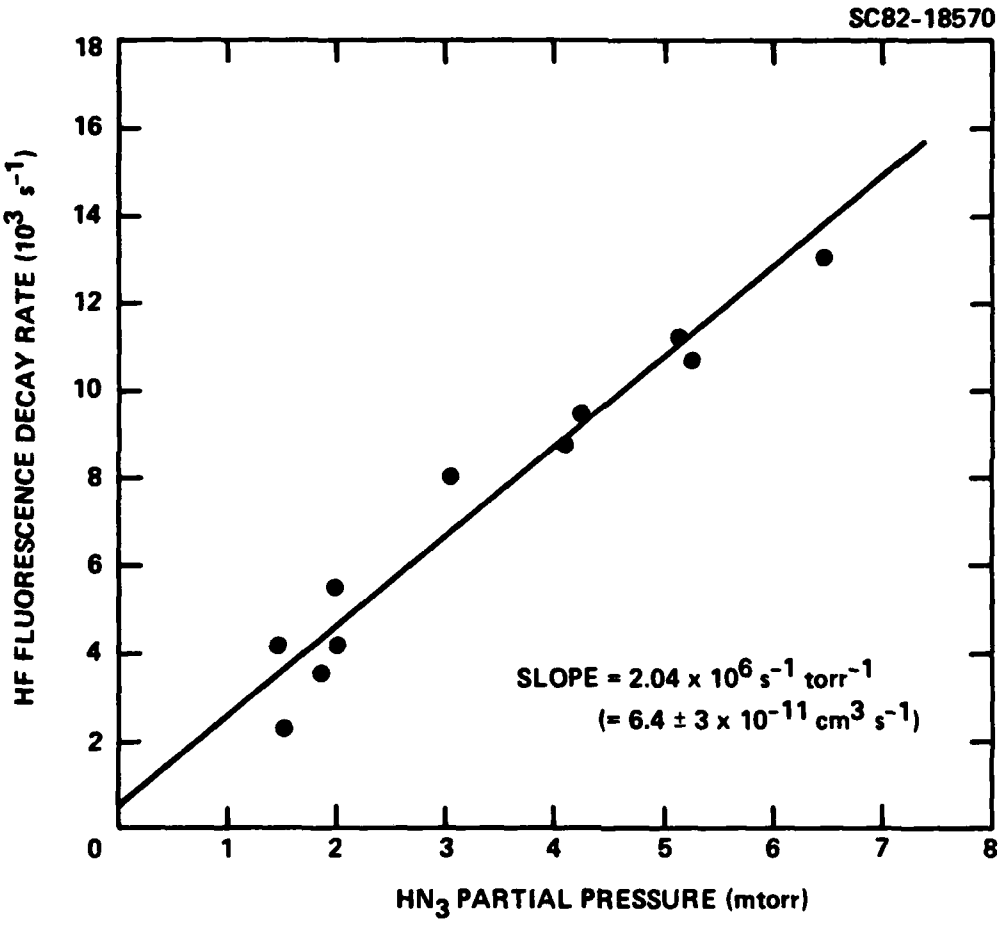

Fig. B3 Plot of the HF fluorescence decay vs HN_3 partial pressure.